

Advanced Ceramics (Self-healing Ceramic Coatings)



Ali Shanaghi, Paul K. Chu, Ali Reza Souri, and Babak Mehrjou

Abstract Advanced ceramics have many commercial applications due to the high corrosion resistance and mechanical properties, but their implementation is frequently compromised by inherent defects including holes, pores, and micro-cracks. The number of coating defects can be reduced by using corrosion inhibitors since the corrosion products help to repair the defects. Small cracks and crevices, of which the internal sources are indistinguishable, can proliferate leading to sudden failure. Therefore, it is essential to develop techniques to identify and monitor cracks so that preventive measures can be taken if the cracks are short and remediable, or a self-healing mechanism can be implemented to enable automatic repair. In this respect, non-automatic repair requires that the defects are first identified, but the process can be difficult and costly. From the perspective of thermodynamics, a system away from thermodynamic equilibrium can be combined with a thermodynamic recovery force such as penetration to return the system to equilibrium. In fact, the regenerative power reduces the entropy to assist the repair processes. Therefore, self-repairing coatings are of great importance and have been progressing gradually from the laboratory to industrial adoption. For example, ceramics-based self-healing coatings containing inhibitors such as organic benzotriazole (BTA) have attracted much interest. Here, different formats of ceramics-based self-healing coatings including titania, zirconia, titanium–alumina, and zirconia–alumina incorporated with benzotriazole (BTA) as an inhibitor are described together with the fabrication processes. By releasing the benzotriazole from titania–alumina–benzotriazole coating, the vulnerable locations for corrosion would be confined and a protective layer is fabricated to enhance the corrosion resistance of the Al 2024 alloy. The amount of BTA plays a vital factor regarding the self-healing efficiency and slow release of BTA is observed to produce the optimal self-healing ability. Titania–alumina coating with 3.6% benzotriazole, provides 76% protection efficiency and the

A. Shanaghi (✉) · A. R. Souri

Materials Engineering Department, Faculty of Engineering, Malayer University, Malayer, Iran
e-mail: alishanaghi@gmail.com

P. K. Chu · B. Mehrjou

Department of Physics, Department of Materials Science and Engineering, and Department of Biomedical Engineering, City University of Hong Kong, Tat Chee Avenue, Kowloon, Hong Kong, China

self-healing behavior of the coating is confirmed by investigating the impedance with immersion time. Moreover, in the $\text{ZrO}_2\text{-Al}_2\text{O}_3\text{-benzotriazole}$ coating, by reaction of oxygen and benzotriazole and subsequently formation of corrosion byproducts, the corrosion resistance and the cathodic reactions would be enhanced and delayed, respectively, lead to an improvement in the properties of double layer. The hardness and elastic modules and plastic deformation of the $\text{ZrO}_2\text{-Al}_2\text{O}_3\text{-benzotriazole}$ coating, decreased and increased, respectively, compared to the coating without the presence of benzotriazole and moreover, the adhesion is the dominant mechanism of wear.

Keywords Self-healing coatings · Inhibitors · Corrosion resistance · Nanomechanical properties

1 Definition of Self-healing

The term “self-healing” in materials science means spontaneous repair of the basic properties of materials after destruction in the external environment. Self-healing is possible in two ways, namely, (1) voluntary (automatic) or without any external interference or (2) involuntarily or with the help of external factors. In some cases, external factors such as the temperature, radiation, pH, pressure, and/or mechanical agents are needed to initiate and maintain the self-healing actions. Some materials have indirect self-healing properties and self-healing materials must be able to repair damage without external forces. At present, self-healing is considered only as mechanical recovery by means of crack repair, but it can be defined as the situation where the small holes and cavities can also be repaired alongside the cracks [1–7]. There are several general means to design self-healing materials: (1) Release of healing agents, (2) Reversible cross-linking, and (3) Exploiting the effects of electrohydrodynamics, conductivity, shape memory effects, nanoparticle migration, co-precipitation, and so on. At present, release of healing agents in the form of particles embedded in the matrix is the most common approach.

2 Release of Healing Agents

Corrosive agents like monomers and catalysts are embedded in the materials during production and if there are cracks, these agents in the reservoirs move to the cracks via capillary force. By the presence of catalysts, they solidify and repair the cracks. This process takes place spontaneously without the need for an external force because the driving force leads to automatic movement and propagation. One of the important methods to embed restoration agents in the matrix is the introduction of micro-reservoirs. Micro-reservoirs retain the solid particles, liquid, or gas droplets in the inner shells that separate and protect them from the surrounding environment [8–14].

3 Principles and Mechanisms of Self-healing in Ceramic Structures

Advanced ceramics such as titania, alumina, zirconia, and composites have many desirable characteristics such as the high-temperature stability, robust strength, high corrosion resistance, special and unique magnetic and electrical properties including piezoelectricity, superconductivity, insulating/semiconducting properties, and so on, which appeal to the industry. In manufacturing of industrial parts, properties such as strength, wear resistance, and anti-corrosion properties are very important. For example, in the chemical industry, strong resistance to acids and other corrosive substances is essential. In the aerospace industry, the heat resistance is critical and in the electronics and communication industry, optical and electrical properties are crucial. In recent years, the widespread use of ceramic materials in the electronics industry, medical technology, and automotive industry has spurred significant development of advanced ceramics as well as ceramic coatings.

Ceramic materials such as alumina, titania, and zirconia have many commercial and practical applications owing to the high corrosion resistance and mechanical properties, but failure can occur due to imperfections including holes, pores, and micro-cracks. Owing to micro-cracks, coatings may lose the protective properties with time. Micro-cracking is initiated by thermal, chemical, and mechanical stress or fatigue, and loss of protective properties exposes the underlying metals leading to corrosion. Repair and replacement of traditional coatings requires physical intervention and so the concept of self-healing has raised enormous interest. Ceramic structures are brittle and can break abruptly. In fact, the fracture toughness of ceramics is not an inherent strength and depends on the fracture toughness and crack geometry. Stress concentration initiated by an applied force can cause crack expansion and fracture at stress level below the fracture stress. In general, two types of surface defects are considered: (1) micro-cracks, cavities, and pores created during production and heat treatment and (2) micro-cracks and cavities caused by penetration of corrosive ions in the corrosion process.

If the small surface cracks, cavities, and pores can be repaired, the strength of the ceramic structure and corrosion resistance can be boosted significantly. According to the types of defects, there are different mechanisms pertaining to the heat treatment in order to repair cracks during production of ceramic materials [15, 16], namely re-sintering, relaxation of the tensile residual stress at the indentation site, and crack bonding by oxidation. The common failure mechanisms in ceramic coatings are (1) nucleation and instantaneous failure of the materials and (2) nucleation, crack development and propagation, and delayed failure. To repair cracks by penetration of corrosive ions, the use of healing agents and creation of corrosion products at defects and cavities are effective. In general, it is necessary to restore the strength of the area by the following means [17–23]: (1) repair done simultaneously with cracking, (2) complete filling of the volume between the crack walls and products, and (3) creating sufficient bonding strength between the products and crack walls.

In a system deviating from the thermodynamic equilibrium, a thermodynamic recovery force such as penetration can revert the system back to equilibrium. In fact, the recovery force raises the local entropy to help the healing process. For example, creation of a supersaturated solid solution leads to the establishment of semi-stable but non-equilibrium conditions. Failure and rupture due to defects such as cracks and so on destabilize the semi-stable conditions to move toward equilibrium. Therefore, coatings have the ability to self-heal when they are in the semi-stable state before surface defects, mechanical damage, or penetration of corrosive agents occur. Two mechanisms can be considered: (1) self-healing through supersaturated solid solutions of the active elements and (2) self-healing through the reaction of monomers and inhibitors in the coatings.

Surface defects, mechanical damage, and corrosive agents can move the coatings from the semi-stable state to the stable state, which is the same as performing a chemical reaction and creating chemical products to repair defects. Recent advances in surface engineering have revealed new avenues to construct active surfaces consisting of a host (inactive) and guest (active) structure. This can be done by inserting the active component into the layered structure so that the inactive component layers contain the active components (such as inhibitors) or by forming tanks (capsules) on the micro- or nano-scale in the coatings to store the active components.

4 Thermodynamics of Healing Processes in Coatings

Destructive processes such as wear, corrosion, fatigue, failure, and creep often involve reactions with different characteristics and different hierarchies on the macro-, micro-, and nano-scale that occur naturally in the system. Friction and abrasion (including contact of abrasive and coarse particles with the micro-, macro-, and nano-dimensions), capillary action, adhesion, chemical bonding [24], and corrosion processes involve different anodic and cathodic ones on the macro-, micro-, and nano-scale. In most cases, these reactions produce irreversible energy loss but in some cases, entropy production at one level such as macro-scale may offset that at another level. Since the processes are independent of the different levels and entropy is a function of the state, the net entropy can be expressed as the sum of the entropies of the system as shown by Eq. (1) [25]:

$$\Delta S_{\text{net}} = \Delta S_{\text{macro}} + \Delta S_{\text{micro}} + \Delta S_{\text{nano}} \quad (1)$$

For example, a homogeneous solid structure, in which the micro-/nanosurface corresponds to atomic vibrations in the crystal lattice, porous structure, grains, defects, and dislocations on the micro-scale, can be considered. A defect-free single crystal has lower entropy (ΔS_{micro}) than a defective structure. Larger defects such as cracks and voids are considered in macro (ΔS_{macro}) components and so materials with regular microstructures or surfaces with distinct textures have smaller entropy (ΔS_{macro}) than micro-structured materials which have irregularities or surfaces with

different textures [25] for defect repair. In fact, it is assumed that macro-scale defects such as cracks and cavities have additional entropy (ΔS_{macro}). The healing process can be accomplished by releasing self-healing agents and breaking the microcapsules. Rupturing microcapsules decreases the microstructural order and increases ΔS_{macro} . When $|\Delta S_{\text{macro}}| < |\Delta S_{\text{micro}}|$, the healing process is gone with a decrease in entropy on the macro-scale and an increase in entropy on the micro-scale. Therefore, according to the macro-scale curing process, the net entropy is equal to the entropy on the macro-scale: $\Delta S_{\text{net}} = \Delta S_{\text{macro}}$. Increasing the order of the structure and decreasing the entropy on the macro-scale can be accompanied by increasing the entropy on the smaller micro- or nano-scale. The structure becomes more orderly, although increased loss and excess entropy on the nano-scale occur each time when grain boundaries propagate [25].

5 Advanced Self-healing Ceramic Coatings

Ceramics-based coatings such as titania, alumina, zirconia, and their compounds have good corrosion resistance, abrasion properties, and hardness but over time, penetration of corrosive ions reduces the ceramic coating adhesion strength to the substrate and consequently reducing the lifetime. The self-healing ability of ceramic coatings prevents penetration of corrosive ions leading to better lifetime and performance in corrosive and harsh environments. In order to create an active or inherent protection state in the coatings, corrosion inhibitors are placed into the coating matrix so that if the coating is damaged and the substrate is exposed to a corrosive environment, the inhibitors can neutralize the metal surface and prevent corrosion reactions. Inhibitors are chemical compounds that in the presence of small amounts in the corrosive environment of a metal, they can reduce the corrosion rate.

5.1 *Types of Inhibitors*

Inhibitors can be organic or inorganic or a combination. Inorganic inhibitors often work by regenerating damaged or anodic areas and forming insoluble deposits. These deposits precipitate and provide a barrier against penetration of electrolytes, water and oxygen. Common inhibitors include phosphates, nitrites, molybdates, tungstates, and chromates [26–29], which are described in the following:

– **Phosphates**

Phosphates and their derivatives are classical inhibitors and their derivatives such as zinc phosphate are well-known corrosion inhibitors that create corrosion products consisting of iron and phosphate compounds that prevent corrosion of steels and reduce cathodic delamination. Other phosphate compounds such as ammonium

magnesium hydrogen phosphate are considered “greener” corrosion inhibitors for protection of epoxy coatings [30].

– Nitrites

Nitrites can prevent pitting corrosion and impose less detrimental effects for the environment than inhibitors containing heavy metals, for example, CrO_4^{2-} , WO_4^{2-} , MoO_4^{2-} , and $\text{Cr}_2\text{O}_7^{2-}$. The electrostatic force between nitrite ions and coatings results in easy reactions with surface compounds, thereby increasing the corrosion resistance by creating corrosion products [31].

– Molybdates

Sodium molybdate, Na_2MoO_4 , as a mineral inhibitor, is highly effective in increasing the corrosion resistance of metals such as steels and its derivatives are considered non-toxic and green inhibitors [32].

– Tungstates

Tungstates constitute one type of environmentally friendly corrosion inhibitors. Among them, Tungstate anions (WO_4^{2-}) have been extensively studied in different corrosive media for active protection [33]. In addition, sodium tungstate can protect metals in neutral, acidic, and alkaline solutions, and is considered environmentally friendly anodic corrosion inhibitors. The inhibition effects of tungstate ions are derived from the formation of iron–tungstate complexes on the surface. However, it is better to avoid using tungstate alone for corrosion protection applications on account of the low inhibition efficiency at low concentrations, in addition to the high cost and poor oxidation ability [33].

– Chromates

Chromates which are effective due to the low water solubility, strong oxidation behavior, and neutral nature of corrosion products are largely used in the aerospace industry and ester pretreatment. However, they pose carcinogenic issues and efforts are being made to replace chromates with more environmentally friendly and safer materials [34].

– Vanadates

Vanadium compounds are non-chromatic corrosion inhibitors. Although vanadate conversion coatings (VCC) are deposited on aluminum alloys, they are about half a micrometer thick and contain a network of cracks. Vanadium compounds work as pigments in the “super-primary” coating system and inhibition arise from the barrier oxide film formation and its deposition by the sol–gel process. This film is insoluble in a wide range of pH and environmental conditions [35].

Organic compounds also have significant applications in surface corrosion inhibition due to good bonding with the surface of materials leading to increased corrosion inhibition, cost-effectiveness, ease of use and synthesis, as well as the possibility of

recycling [36]. Organic compounds including aliphatic and aromatic amines such as ethylene diamine, ammonia, cyclohexylamine, benzylamine, aniline, methyl aniline, dimethyl aniline, phenylhydrazine, phenylamine, and ortho- and para-toluidin prevent corrosion by the formation of an adsorbed layer on the metal surface [37]. The prerequisite for organic inhibitors to be effective is attachment to the metal surface. They also work by increasing the local pH and neutralizing the substrate. Organic inhibitors have been reported to reduce and minimize corrosion when the corrosive medium contains dissolved oxygen, salts, and weak acids. When the corrosive environment consists of strong acids such as hydrochloric acid and is subject to a high temperature and microbial activity, polar organic compounds and colloidal organic matters are better inhibitors against corrosion [38]. Among the various organic inhibitors, heterocyclic compounds are of considerable importance as they adsorb heterocyclic compounds on the surface to prevent corrosion reactions. Heterocyclic compounds make use of their electron-rich centers such as polar functional groups including $-\text{NHMe}$, $-\text{NH}_2$, $-\text{NMe}_2$, $-\text{OH}$, $-\text{NO}_2$, $-\text{OCH}_3$, $-\text{O}-$, $-\text{CN}$, $-\text{CONH}_2$, COOC_2H_5 , etc., as well as π -electrons of the hetero-species such as $\text{NC}=\text{O}$, $\text{NC}=\text{N}-$, $\text{NC}=\text{S}$, $-\text{C}\equiv\text{N}$, $-\text{N}=\text{O}$, and $-\text{N}=\text{S}$, and homo-species including $\text{NC}=\text{C}$, $-\text{N}=\text{N}-$, and $-\text{C}\equiv\text{C}-$. Compounds with a larger molecular size are better corrosion inhibitors than smaller compounds because they cover a larger surface [36]. In the following section, common organic inhibitors used in the industry are described.

– Azoles and Thiazoles

Azole and thiazole inhibitors contain nitrogen and sulfur donor atoms and form suitable compounds with metal cations with polymeric properties as surface oxidation barriers. The inhibitory properties of azoles stem from physical or chemical adsorption via formation of single molecular layers. Much work has been done on the application of 1,2,3-benzo-triazole (BTA), 2-mercapto-benzothiazole (MBT), and their derivatives as corrosion inhibitors [39].

– Imidazole

Imidazole-based imidazole carbonitriles which are heterocyclic compounds containing two nitrogen atoms (diazole) in the ring have biological and industrial applications. The imidazole ring is contained in histamine, histidine, antifungal, and antibacterial drugs, antibiotics, and midazolam. By introducing an appropriate substitute into the five heterogeneous rings of imidazole, its properties can be modified and its easy dissolution in water can be achieved. Imidazole interacts strongly with charged metal surfaces due to its flat geometry and high bipolar torque. When an imidazole contains a hydrophobic chain in its structure it's the most effective inhibitors and electrochemical studies show that increased hydrophobicity raises the conservation efficiency [36].

– Pyridine

Carbonitrile pyridine is a six-member heterocyclic compound that contains one nitrogen atom in the heterocyclic ring. It is a flammable, water-soluble, and basic

liquid. This compound can be found in vitamins, pharmaceuticals, and agrochemicals and pyridine with high aqueous phase solubility shows the robust affinity to interact with a metallic surface [36].

– Nitro Compounds

Nitro compounds have at least one nitro group in the molecular structure to attract electrons, and their presence in organic inhibitors reduces the anti-corrosion effects. However, replacement of NO_2 with one nitrogen atom and two oxygen atoms in the smaller molecules increases the molecular size. $-\text{NO}_2$ being highly polarized reacts strongly with polar electrolytes and dissolves complex molecules that normally do not dissolve without $-\text{NO}_2$, consequently enhancing the inhibitory effects [36].

– 8-Hydroxyquinoline (8-HQ)

8-Hydroxyquinoline (8-HQ) is one of the common corrosion inhibitors due to this fact that the small molecule 8-HQ has strong bidentate chelating ligand for metal ions. The structure consists of a nitrogen and oxygen atoms as donor atoms to complex of metal ions. Recently, 8-HQ has been incorporated as a corrosion inhibitor into self-healing and smart coatings [40].

Important factors regarding the long-term corrosion protection are the corrosion inhibitors concentration in the coating and the barrier properties of formed self-healing layer in the defect sites. Other factors such as solubility may have an impact on self-healing as a low solubility of the corrosion inhibitor reduces the amount of active agents in the damaged areas in the coatings. However, a high solubility causes rapid removal of active compounds from the coatings giving rise to only short-term protection [41, 42]. Inhibitors can react chemically with the components of coatings and in some cases, the barrier properties of the coatings are destroyed [43].

The release of inhibitor from the self-healing coatings should be fast enough to respond to changes in the environment or status of the coatings quickly. There are new strategies to produce self-healing coatings, for example, by combining nano-scale containers (carriers) with active barrier components in conventional coatings. This method produces new coating systems based on passive–active structures. In fact, nanoreservoirs which are evenly distributed contain active inhibitors to eliminate excessive deterrence and remove osmotic bubbles when the inhibitory salts are highly soluble or have a very small particle size.

When local changes in the environment or the corrosion process occur in the coating defects, nanoparticles respond to these signals and release active materials [44, 45]. The inhibitor loading mechanism in self-healing ceramics-based coatings is via incorporation of oxide nanoparticles as nanocarriers on which the inhibitors adsorb. Oxide nanoparticles are also considered coating enhancers and their addition improves the inhibitory properties [46–50]. In addition to increasing the corrosion resistance, adding a corrosion inhibitor to oxide nanoparticles creates the self-healing ability. For example, stabilization of an inhibitor such as Ce^{3+} on the surface of ZrO_2 nanoparticles during hydrolysis of the zirconia sol produces a hybrid nanocomposite coating containing oxide nanoparticles with cerium ions [51–53]. The small diameter

of the oxide nanoparticles increases the carriers surface area and increases the loading capacity of the inhibitors. Consequently, long-term release of the inhibitor from the nanoparticle surface improves the corrosion behavior.

5.2 Self-healing Ceramics-Based Coatings Preparation Methods

In general, several processes can be used to produce self-healing coatings containing barriers, including (1) use of inhibitor containers, and (2) incorporation of an inhibitor directly into the coating. The use of inhibitory containers in polymer-based coatings is divided into multiple groups depending based on the organic or inorganic containers type [54].

5.2.1 Organic Containers

In this case, the inhibitors in micro or nano-organic containers are self-healing epoxy coatings. Researchers have tried to examine the impacts of various organic nanocontainers as well as their other properties such as size, shape, and location in epoxy coatings. These nanoenclosures contain anti-corrosion inhibitors improve the corrosion resistance of materials. In this process, the inhibitor is placed inside the chambers, followed by active ingredients released to the damaged area freely due to mechanical damage or pH change leading to improved corrosion resistance. Various parameters such as the diameter of the chambers and amount and distribution of the inhibitors in the coating affect the inhibitor release rate and the efficiency of the self-healing coating. Organic containers are cellulose nanoreservoirs and polymeric microcapsules. While cellulose nanoreservoirs are used, the epoxy matrix with a grid structure is preferred for better repair. Cellulose chambers improve the thermal mechanical properties of the epoxy matrix by creating lattice structures rendering them excellent reservoirs in self-healing coatings. Another effective and practical approach to protect the metal surface is using the polymer microcapsules loaded with inhibitors as they can release the inhibitors in a controlled manner. This method is quite common and the polymer capsules can be made from urea formaldehyde (UF) resins via polymerization techniques. The facile preparation steps with high degree of control on the microcapsule size and the shell thickness are the main advantages of the in situ micro-polymerization methods [54].

5.2.2 Inorganic Containers

Halloysite nanotubes (HNTs), titanium dioxide (TiO₂), and mesoporous silica are used to hold inhibitors for self-healing purposes. These fillers internally carry on the

self-healing liquids can act as a reservoir. Due to the larger aspect ratio (L/D) ratio of TiO_2 and HNT compared to the polymeric nanocontainers, they can cover larger site on polymer matrix. Furthermore, this system significantly enhances the overall thermomechanical properties. Encapsulation of inhibitors in organic containers is an easy process and the layer-by-layer (LbL) approach is a suitable approach to achieve the self-healing epoxy coatings. The reservoirs regulate inhibitor loading and release, and additionally, the multilayer permeability of the system can be governed by factors like the temperature, pH, electromagnetic field, and ionic strength [54].

The aforementioned methods are applied to create self-healing polymer-based coatings containing inhibitors, but cannot be used for ceramics-based coatings or in the attempt to reduce adhesion of ceramic coatings. In the ceramic base coatings, direct use of a barrier by solution processes such as sol-gel can produce a homogeneous and uniform coating with the suitable distribution of the barrier in the ceramic-based coating.

5.2.3 Sol-Gel Coatings

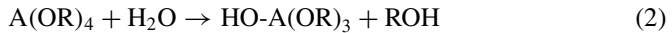
There are various methods to deposit coatings on metals, for example, physical vapor deposition (PVD), chemical vapor deposition (CVD), electrical deposition, plasma spraying, and sol-gel process. The sol-gel process is one of the common techniques to synthesize homogeneous powders, coatings, and ceramic composites and has many advantages [55, 56]. It is a low-temperature process (close to room temperature) and so thermal evaporation and degradation of organic inhibitors are minimized. Since liquid precursors are utilized in this process, it is possible to form coatings with a complex shape and there is no need to melt or machine in order to produce the thin films. The sol-gel process is environmentally friendly and final rinsing is usually not required.

In the sol-gel method, an oxide network is prepared by continuing compression of the precursors in the liquid medium [55–57] and in general, sol-gel coatings can be prepared in two methods, namely, the inorganic or organic method. In the inorganic methods, a colloidal suspension (normally the oxide format) and the sol coagulating (suspension of colloids with particle at very small sizes, 1–100 nm) are formed to deform the network till a network can be shaped in the continuous liquid state. The organic method is more common which normally begins with a monomer metal-solution or metal-like alkoxy precursor $\text{M}(\text{OR})_n$ in alcohol or other organic solvents with low molecular weight. Here, M represents the main element such as Si, Ti, Zr, Al, Fe, and B and R stands for the alkyl group ($\text{C}_x\text{H}_{(2x+1)}$).

The sol-gel process consists of four stages: (1) hydrolysis, (2) formation of chains and particles through densification and polymerization, (3) particle growth, and (4) polymer structure agglomeration and subsequent network formation that spreads throughout the liquid environment followed by its thickening to form the gel-like structure. Hydrolysis and compaction occur simultaneously at the beginning of the hydrolysis reaction and the products with low molecular weight such as alcohol

and water can be formed after drying and contraction of the lattice causes more compaction [55–58].

Metal alkoxides (Ti, Zr, Ce, Al, Si, etc.) with the typical formula of $A(OR)_4$, where A, OR, and R stand for a metal atom, an alkoxy group, and alkyl ligand, respectively, are considered as the precursors for the sol–gel process. The typical reaction of alkoxides in contact with water is shown by Eq. (2) (hydrolysis) [59]:



According to Eqs. (3) and (4), hydroxyl ions bind with atom A to form alcohol and partially hydrolyze the starting materials, which are then combined by condensation:



Reactions (3) and (4) are the polymerization process in gelation in which the solid network contains the liquid phase in the cavities and continues to build the network containing the O-A-O connections.

The rate of hydrolysis is usually larger than that of condensation. The metal alkoxides reactivity is different and increases in the form of $Ce(OR)_4 > Zr(OR)_4 > Ti(OR)_4 \gg Si(OR)_4$. In some cases, due to very slow rate of alkoxides reaction with water, catalyst should be used to enhance the rate of process. Acidic catalysis is commonly used to form coatings. Some of the determining factors which make an impact on hydrolysis and condensation are the ratio of water to alkoxide, pH, temperature, concentration of reactants, and nature of the alkoxide groups. Changes in these parameters affect not only the kinetics of the sol–gel process but also the microstructure and nanostructure of the final product [50]. Among the sol–gel coatings, the hybrid one, is more usual compared to the inorganic ones for protection of metal surface from corrosion, based on two facts. Firstly, a thin crack-free micrometer layer can be formed with low oxide-layer sintering temperature (below 100 °C) and secondly, they can provide higher degree of flexibility when mixed with anti-corrosive agents such as inhibitors, pigments, etc.; therefore, it can be said that they can provide higher and better corrosion protection.

Spin coating and dip coating are the most two common techniques for applying the sol–gel coatings to the surface of metals. Spraying and electrical deposition have also been reported. Regardless of the method, after deposition of the coating, evaporation of a large amount of solvent and water leads to significant volume shrinkage and creates internal stress. The film fabrication conditions should be precisely adjusted, otherwise, the internal stress can produce cracks. Usually, curing and heat treatment steps are performed on sol–gel coatings depending on the microstructure, quality, and application [55–58].

5.3 Titania-Based Self-healing Coatings

Titanium (titanium oxide) has very good properties such as chemical stability, thermal resistance and low electron conductivity and TiO_2 is a very good anti-corrosion agent. However, there are not many reports on the application of TiO_2 films as a steel protective coating. CeO_2 has comparable properties, and it has been used in sol-gel fabricated coating with the role of corrosion inhibitor, although it has a wider range of applications in optics, catalyst chemistry, pigments, etc. The oxide layers with more than one component can perform better to protect steel-based materials from corrosive medium and consequently their range of application can be expanded [60–62].

The TiO_2 -benzotriazole nanostructured hybrid sol-gel coating consisted of 1.4, 2.8, and 4.2% benzotriazole, applied on the 7075 aluminum alloys substrates by the sol-gel method. Alkoxide $\text{Ti}(\text{OCH}_2\text{CH}_2\text{CH}_3)_4$ precursor with long chain lengths and miscibility with organic solvents on the molecular level generates crack-free films and organic inhibitors such as benzotriazole has a more homogeneous reaction by alkoxide compounds resulting in better release of the inhibitor to defects for healing [60–62].

Upon usage of benzotriazole, robust complexes can be formed when it reacts with transition metals and consequently, it can enhance the quality of protection of copper-based alloys. Also, it has applications in other sectors such as deicing agents, antifreeze and brake fluids, lubricating oil, and within cooling systems. Furthermore, the corrosion behavior of Fe in brine solution can be improved by using benzotriazole and some of its compounds. In this case, inhibitory effectiveness subjects to its concentration as here insoluble complexes formation protects the surface of metal [60–63].

3-Glycidoxypropyltrimethoxysilane (GPTMS) with its two functional groups, glycidoxy (organic component) and silicon alkoxide (inorganic component), already showed its potential to establish better connectivity among the organic and inorganic compounds in the sol-gel method. Therefore, it can be used to make a network by reaction of glycidoxy group with the both organic and inorganic inhibitors, during the polymerization process. Moreover, a network can be made via hydrolysis for subsequent condensation reactions between SiO and titanium alkoxide [64–66]. Thus, the reaction can be seen between organic groups together compared to the organic and inorganic ones. There are studies regarding the inhibiting action of organic compounds like benzotriazole on aluminum alloys. Usually, it happens with polymeric coatings with the self-healing ability and the thickness between 10 and 100 μm , although it can be too much for some purposes. The thickness of ceramics-based coatings prepared by the sol-gel method is 1–10 μm with 1.2, 3.6, and 4.8% benzotriazole as the self-healing agent [60–62]. Structure and morphology of the TiO_2 nanostructured and its self-healing coating contained different benzotriazole concentrations are shown in Fig. 1, which indicates that adding benzotriazole formed a uniform and homogeneous structure with less micro-cracks compared to the titania nanostructured coating [60].

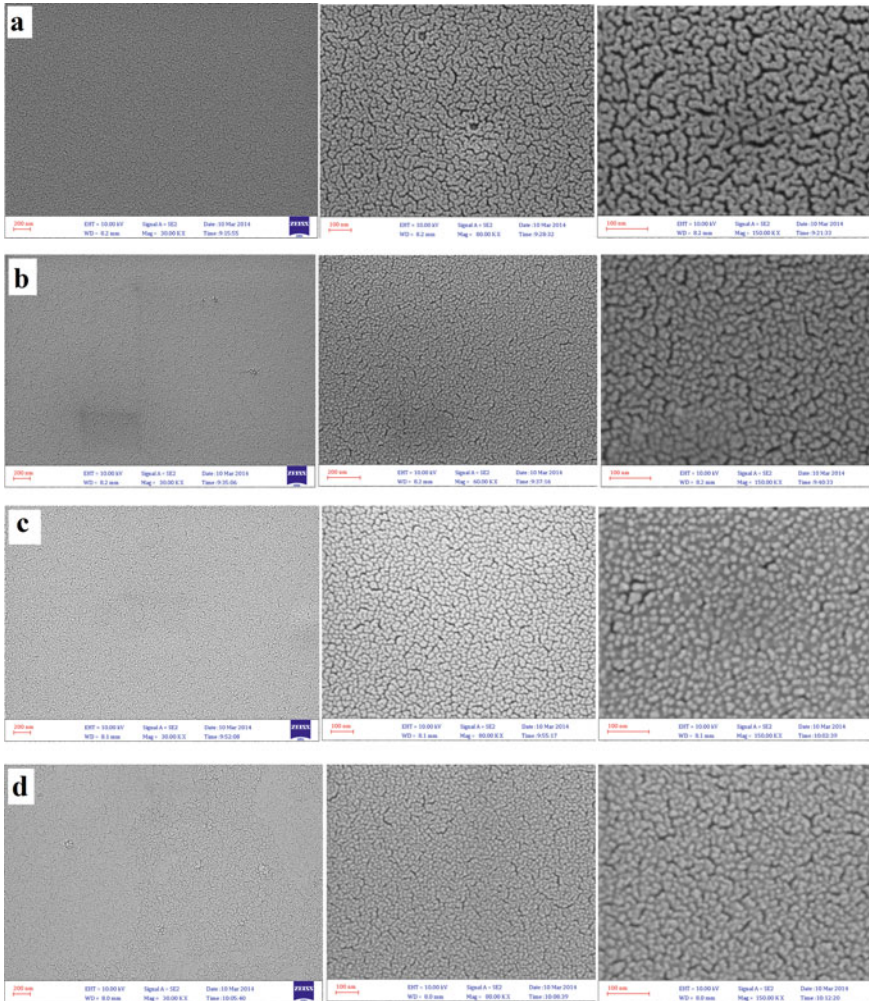


Fig. 1 FE-SEM images of **a** TiO₂ nanostructured, **b** TiO₂-1.4% benzotriazole self-healing, **c** TiO₂-2.8% benzotriazole self-healing, and **d** TiO₂-4.2% benzotriazole self-healing coatings, which are heat treated for 2 h at 150 °C of a heating rate of 1 °C/min. The magnifications of 30, 80, and 150 kX are shown in [60]

When the TiO₂ nanostructured coating was applied on the surface of 7075 Aluminum alloy, the corrosion behavior was deteriorated compared to the uncoated one, according to the results acquired from the Nyquist and bode-phase plots after samples were being immersed in 3.5% brine solution for 24 h (Fig. 2). However, the TiO₂ coating containing the benzotriazole showed higher corrosion resistance. The coating with 4.2% benzotriazole, showed better corrosion resistance compared to the ones with 1.4 and 2.8% due to its homogenous and uniform properties and

also higher compactness of the coating as the defects can be filled out by releasing of benzotriazole. As it can be seen in Fig. 2, the sample containing 4.2% benzotriazole has two time-constant compared to the ones with 1.4 and 2.8%, showed that the corrosion reactions happened at the both coating and its interface with the substrate. It was shown that the inhibitor enhanced the corrosion resistance of TiO₂-4.2% benzotriazole upon immersion for 24 h. When the healing agent was released and subsequently reacted with the medium, a layer was formed between TiO₂ and the aluminum substrate and reduced the effect of corrosive agents, thus enhanced the corrosion resistance of the coating. According to the graphs, by increasing the benzotriazole content from 2.8 to 4.2%, protective layer was formed at higher frequencies. All in all, it can be said that, at both 2.8 and 4.2% benzotriazole, a protective layer was formed, due to releasing of benzotriazole at enough amount, however, the quality of the layer formed from the sample containing 4.2% benzotriazole was better, showed by its better stability and density [60–62].

Releasing of benzotriazole and its subsequent reaction and defects filling enhanced the protection against localized corrosion at low frequencies and among the samples, the coating with 2.8 and 4.2% of benzotriazole provided better corrosion resistance compared to the other groups, the uncoated aluminum substrate, coated with TiO₂ nanostructured and the one with 1.4% benzotriazole. Although the aluminum substrate, 7075, has good resistance to localized corrosion, however, by introducing

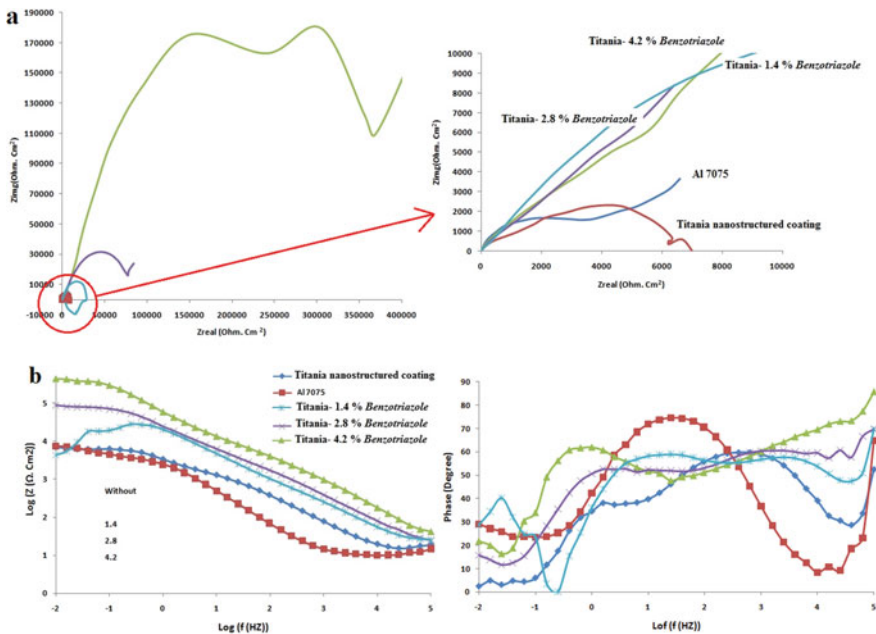


Fig. 2 a Nyquist plot and b Bode-phase plot of the Al 7075 alloy, titania nanostructure coating and titania nanostructured coatings containing 1.4, 2.8, and 4.2% benzotriazole after immersion for 24 h immersion in the 3.5 wt.% NaCl solution [60]

the TiO₂ nanostructured to the substrate, the corrosion resistance would be increased. Therefore, by coating the substrate with TiO₂ nanostructured and TiO₂-1.4% benzotriazole, the resistance to localized corrosion would be decreased as it can be understood from the Bode-phase plot, by the reduction of phase angle and its subsequent shifting toward the zero. But this deficiency can be improved by increasing the benzotriazole content from 1.4% to 2.8 and 4.2% [60–62]. Also, enhancement of localized corrosion resistance of the coating with TiO₂-4.2% benzotriazole can be achieved by increasing the immersion time to 120 h (Fig. 3) due to this fact that the absorption layer formed at the interface of coating and solution, has the higher stability. Extending the immersion time at 3.5% brine solution would decrease the corrosion and specifically localized corrosion resistance of TiO₂ nanostructured coating, however, by adding the healing agent the corrosion behavior, both locally and generally, improved significantly [60–62, 67]. Thermodynamically study of absorption and formation of protective layer between the medium and coating showed that by releasing benzotriazole from the coating with 4.2% concentration, and the subsequent reactions of nitrogen and oxygen molecules with water, an insulating layer was formed [60–62, 67].

Two mechanisms are involved in enhancing the corrosion resistance of the coating with 4.3% of benzotriazole:

- (a) Blocking the surface defects via corrosion by-products, due to release of inhibitor and its subsequent interaction with the molecules and ions in the environment,

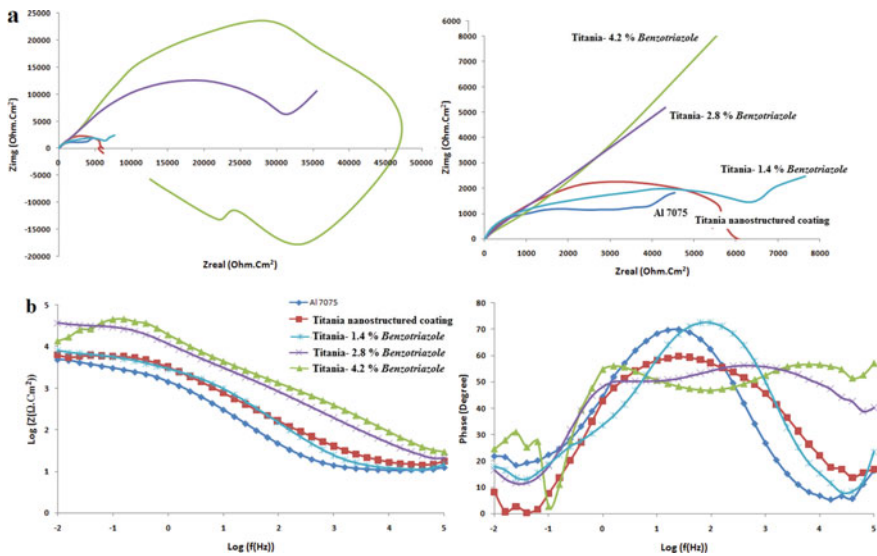


Fig. 3 a Nyquist plot, and b Bode-phase plot of the Al 7075 alloy, titania nanostructured coating, and titania nanostructured coatings containing 1.4, 2.8, and 4.8% benzotriazole after immersion for 120 h in the 3.5 wt.% NaCl solution [60]

- (b) Formation of insulating layer between the coating and the medium due to the release of inhibitor and its surface adsorption.

Although it's been said that the benzotriazole released from the coating produces defects in the coating to ultimately reduce the resistance to the corrosion, both locally and generally, however, it is shown that the presence of 4.2% of benzotriazole in the coating can improve the corrosion resistance and healing reactions in the TiO₂ nanostructured coating.

5.4 Titania–Alumina Self-healing Ceramics-Based Coating

Titania and alumina coatings are protective coatings against corrosion and nanoparticles of titanium dioxide have anti-corrosion properties. Although titania is an active compound for the catalytic activity, the small surface area and change of the structure at elevated temperature (e.g., instability of the anatase structure) are limitations. Studies have been conducted to enhance the anti-corrosion properties by combining titanium oxide with other oxides [62, 68–70]. Alumina (produced by sol–gel technique) is structurally stable and has a large specific surface area [71, 72]. Alumina also has a good oxidation resistance to abrasion and provides excellent corrosion resistance [73].

After preparing the titania solution, the tri-butyl aluminum precursor is used as an alumina source to prepare the alumina solution. The solution containing 80% of the titanium solution and 20% of the alumina solution is added to tri-methoxy-silane as an encapsulate liquid to prepare benzotriazole solutions with three different concentrations [62]. According to FE-SEM image (Fig. 4), a more homogenous and smoother composite coating of titania-alumina containing benzotriazole can be achieved compared to the ones without it. benzotriazole reduces adhesion among particles. As shown in Fig. 4a, nanoparticles attached together with poor connection to each other can create cracks with small size and micro-channels. The stress caused by shrinkage upon the heat treatment and solvent removal can induce the crack formation. The corrosion rate can be increased due to more cracks formation, however, on the other hand, more benzotriazole can be stored in them. In this regard, by adding 1.2% benzotriazole, the cracks surface can be covered, and smoother and more homogenous structure can be achieved compared to the case without any benzotriazole. By further increasing the content of benzotriazole to 3.6%, as more cracks would be filled therefore, the homogeneity of surface structure would be enhanced. However, there is an optimal concentration regarding the application of benzotriazole to fill out the cracks, as increasing its content to 4.8%, a coating with higher porosity would be formed [62].

The coatings properties such as strength and adhesion are affected by the surface structure. For example, the amount of TiO₂ cracks deposited on Al 2024 alloy can be reduced by alumina [74, 75] and also higher surface roughness can induce more cracks [76–78]. The roughness and thickness of TiO₂–Al₂O₃ composite coatings are

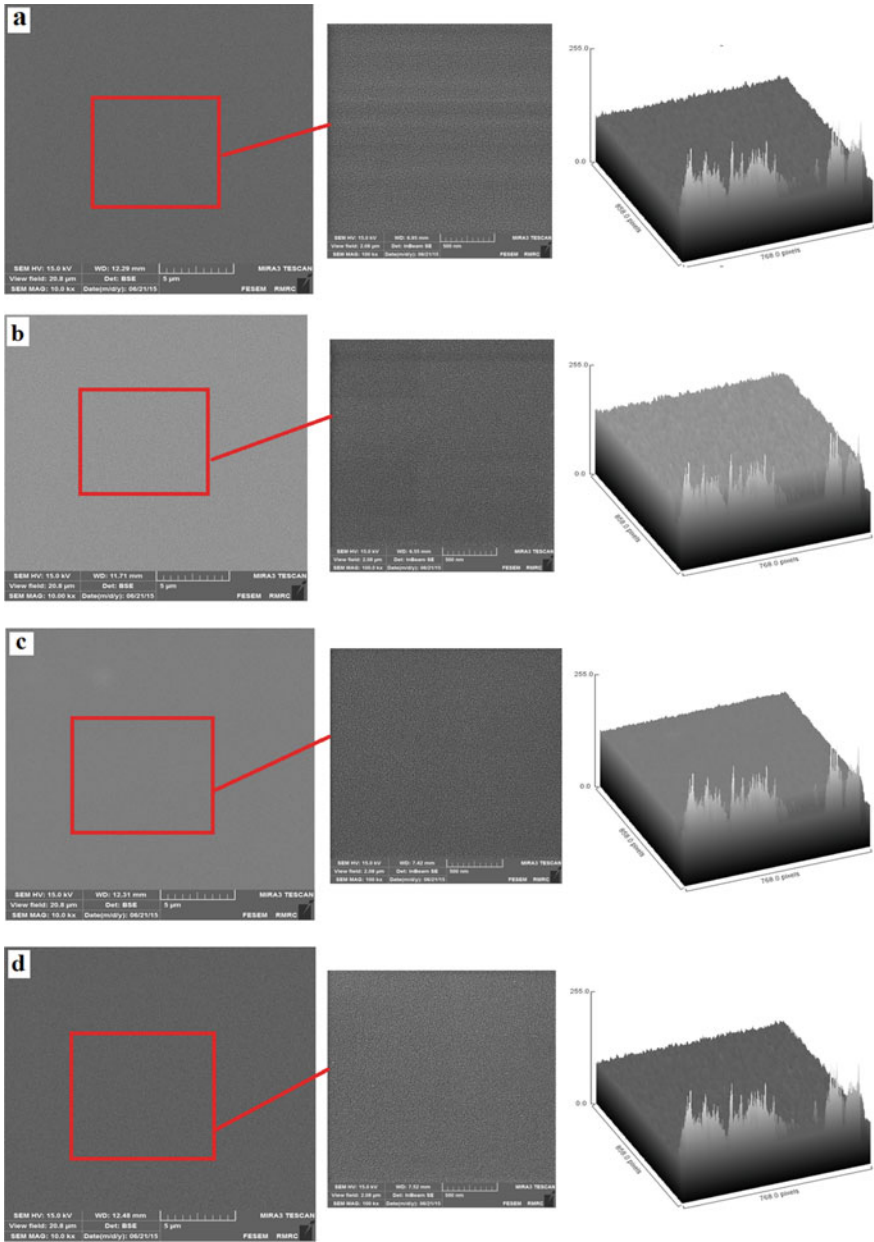


Fig. 4 FE-SEM images of the TiO₂-Al₂O₃ coatings: **a** Without benzotriazole; **b** 1.2% benzotriazole; **c** 3.6% benzotriazole; **d** 4.8% benzotriazole (10,000X and 100,000X magnification) [62]

summarized in Table 1. Upon the introduction of 1.2% of benzotriazole, the surface roughness (Ra) is increased, however, by further increasing the concentration of benzotriazole to 3.6 and 4.8%, better consistency can be attained. As you can see in Table 1, by adding more than 1.2% benzotriazole, lower surface roughness compared to the ones without the inhibitor can be achieved. The bonding quality between the Al 2024 substrate and the coating is affected by the mismatch of thermal expansion coefficient. The stress generated during the heat treatment can be accumulated and reduce the bonding strength of the coating as the thermal contraction and coefficient behavior of the coating and substrate is different [79]. In this regard, the role of alumina and benzotriazole is reducing the crack formation and increasing the bonding strength of the substrate and ceramic coating. The benzotriazole diffuses into the cracks upon its formation and probably reacts there and finally heals the defects. It should be noted that by further increasing the concentration of the benzotriazole to more than 4.8% the coating bonding strength would be decreased and delamination can be happened more easily in the ceramic coatings [60–62].

To study the coating corrosion behavior, they were immersed in the NaCl solution with 3.5 wt.% up to 96 h. It was found that when the immersion time was increased from 1 to 48 h, Fig. 5a–b, the polarization and corrosion resistance is increased. Compared to the coating only containing $\text{TiO}_2\text{-Al}_2\text{O}_3$, reactants attach to the surface, and due to redox reactions, the ion exchange happens among the chloride ions in the electrolyte and the ones in the coating and finally reduces the charge transfer resistance (1 h immersion (Fig. 5a)). By increasing the immersion to 48 h (Fig. 5b), corrosion produces filled the cracks and made a barrier to the transfer of ion to the metal surface. From the linear section, it can be understood that the system is governed by the movement of reaction products or reactants from the metal surface toward the medium. This is the case when the reaction products cover the metal surface [80]. Followed by 96 h immersion (Fig. 5c), a higher concentration of chloride ions and a gradual reduction in the passive film resistance, formed on the top of the corrosion byproducts can be seen. It is shown that the polarization resistance of the coatings with benzotriazole content of 1.2 and 4.8%, at 1 h is higher than 48 h. Trimethoxysilane ($\text{C}_3\text{H}_9\text{OSi}$, coupling agent) by forming a membrane around

Table 1 Surface roughness (Ra) and thickness of the $\text{TiO}_2\text{-Al}_2\text{O}_3$ coatings containing 1.2%, 3.6%, and 4.8% benzotriazole [62]

Sample	Ra (nm)	Thickness of one layer (nm)	Total thickness after five times immersion (μm)
Titania–alumina coating (no benzotriazole)	20.45	450	2.25
Titania–alumina coating (1.2% benzotriazole)	0.14	510	2.55
Titania–alumina coating (3.6% benzotriazole)	0.03	600	3.00
Titania–alumina coating (4.8% benzotriazole)	0.19	640	3.20

benzotriazole acts as a bridge between benzotriazole (an organic inhibitor) and $\text{TiO}_2\text{-Al}_2\text{O}_3$ (minerals). Benzotriazole can be released by variation of the pH or scratching and form a thin layer to protect the corroded metal from the diffusion of corrosive agents. The inhibition efficiency depends on two factors, adsorption of the inhibitor on the surface of metal and its inhibition efficacy at the metal–solution interface [62, 81].

As the polarization resistance is still low after 1 h of immersion, it can be concluded that the molecular absorption on the surface of Al substrate hasn't yet been completed and the equilibrium state between the molecules in the solution and absorbed on the surface is not yet reached. The inhibitory effect of benzotriazole is associated to the BTAH adsorption to the surface of Al substrate and formation of $[\text{BTA}]_{\text{ads}}\text{-Al}$ layer. This process happens by the removal of H from BTAH and subsequently formation of BTA^- and its linkage to the Al ions and the formation of $[\text{BTA}]_{\text{ads}}\text{-Al}$ layer on the surface. [81, 82]. This process is subjected to various factors and the physical and chemical properties of inhibitor molecules like functional groups, electron density, π orbitals, as well as charged metal surface [82–84].

Benzotriazole improves the coatings corrosion resistance compared to the ones without any inhibitor molecules after 1 h immersion (Fig. 5a). However, it should be considered that by adding 1.2% benzotriazole, no improvement in corrosion resistance can be seen after 48 h immersion (Fig. 5b) and at the inhibitor concentration below than the critical value, corrosion behaviors are worsen compared to the ones without any inhibitor at all. The pitting deteriorates the corrosion behavior by breaking the passivation and reduces the anodic area compared to the cathodic one. Adding below than optimal concentration of benzotriazole, enriches the porosity and consequently damages the protection behavior, thus a critical point for the amount of benzotriazole to protect the surface should be considered [81]. Here in this study, it is found that the optimal concentration of benzotriazole is 3.6% as it showed better polarization resistance compared to the one with 4.8%. The constructive or destructive impacts of benzotriazole on protective behavior of the prepared coatings with sol–gel techniques hinge on various factors including, composition of sol, deposition parameters and the benzotriazole concentration in the sol part. An important factor to provide the stability in the corrosive medium is the corrosion protection behavior for a long term and to provide the long-lasting corrosion protection, factors such as the corrosion inhibitors concentration, the silica film structure, and the self-healing layer barrier property formed in the flaws should be carefully considered. Moreover, there are some other factors which can impact the self-healing properties like the solubility behavior of corrosion inhibitors in the corrosive medium. For instance, low solubility of the corrosion inhibitors causes active agents depletion from the affected area, however, high solubility can lead to fast leaching [81]. The polarization curves of the titania–alumina composite coatings with 1.2, 3.6, and 4.8% benzotriazole after immersion in 3.5 wt.% NaCl solution for 96 h are shown in Fig. 6, and the results, such as corrosion current density (i_{corr}), anodic slop (β_a), cathodic slop (β_c), corrosion potential (E_{corr}), passivation current density (i_{pass}), and inhibition efficiency (η_p), are summarized in Table 2. This table shows that when the concentration of benzotriazole increased from 3.6 to 4.8%, the corrosion current

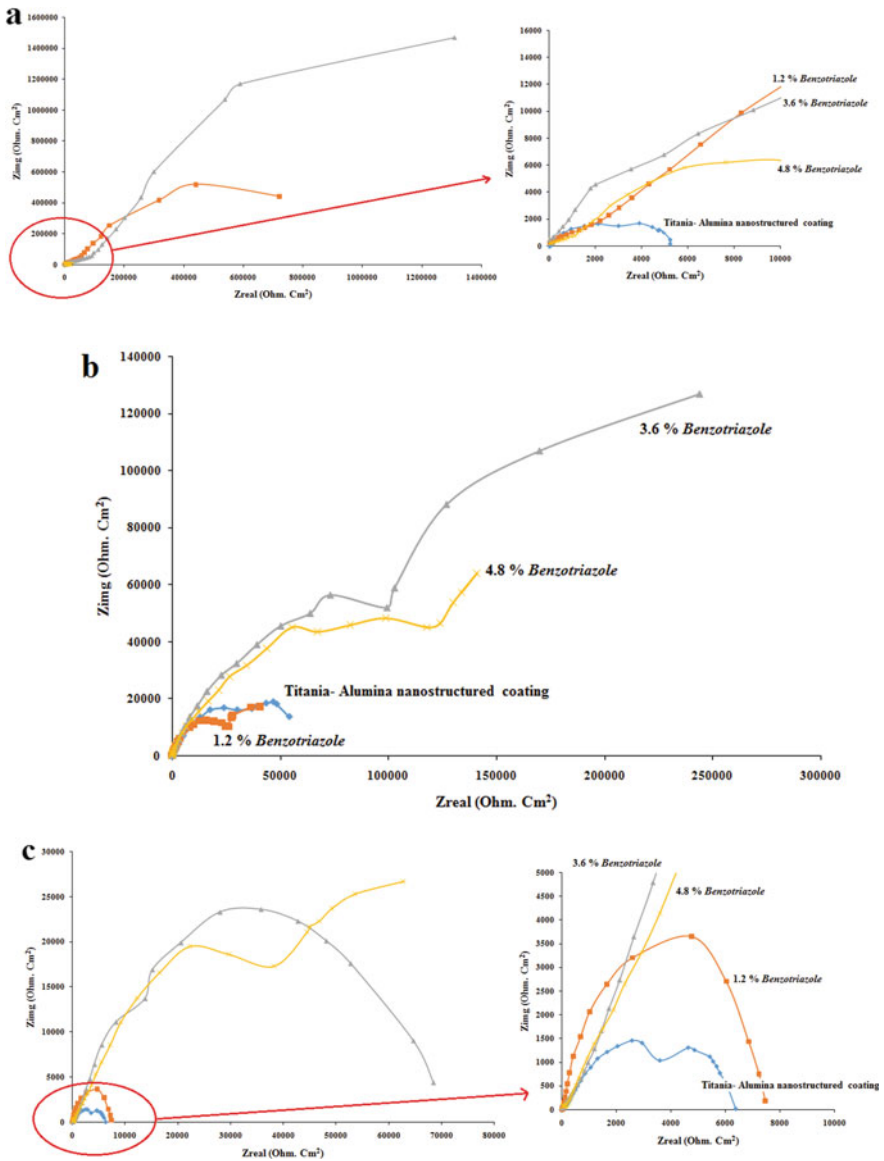


Fig. 5 Nyquist plots of Al 2024 alloy with the TiO₂-Al₂O₃ coatings: No benzotriazole, 1.2% benzotriazole, 3.6% benzotriazole, and 4.8% benzotriazole after immersion in 3.5 wt.% aqueous NaCl for **a** 1 h, **b** 48 h, and **c** 96 h [62]

density was decreased compared to the case of coating with 1.2% or even without any inhibitor, where the corrosion current is the current produced while electrochemical corrosion is occurring, and electrons move from the anode to the cathode. Probably, by increasing the benzotriazole content, more corrosion sites are blocked. The coatings with 3.6% benzotriazole, shows the self-healing ability. The coating and polarization resistance would be decreased when the corrosion reactions happen in the defects during the immersion. In the case of the sample with 3.6% benzotriazole, its slow release from the coatings when exposed to the solution and probably the passivation of defects, produces the self-healing property. However, passivation area of anodic branch experienced some oscillations. Casenave and Coll [85] by studying the aluminum corrosion in the presence of benzotriazole showed the benzotriazole suitability as a cathodic inhibitor. Other studies have named anodic and/or cathodic inhibitors [53, 64] and it is shown that the inhibitory mechanism of BTAH is related to its adsorption to the Al surface and subsequent formation of [BTA]ads:Al layer [62, 81].

Finally, it should be said that the benzotriazole concentration is a main factor regarding the self-healing properties of the coating as its steady release, specifically in the case of 3.6%, when exposed to an aqueous solution, render the self-healing ability. Also, elevated polarization resistance can be stemmed from the defects passivation. However, as there is a race between corrosion and healing process, oscillations can be seen in the cathodic branch of passivation area. The coating with 3.6% benzotriazole can provide the highest protection efficiency of 76% [62].

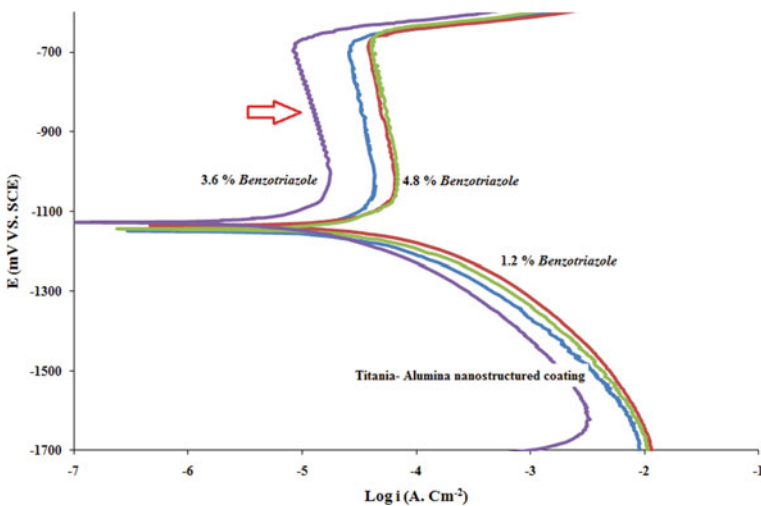


Fig. 6 Polarization curves (electrode potential versus the logarithm of the current density) of the $\text{TiO}_2\text{-Al}_2\text{O}_3$ coatings without benzotriazole, and with three various benzotriazole concentrations after being immersed in 3.5 wt. % NaCl solution for 96 h [62]

Table 2 Acquired data from polarization tests of the $\text{TiO}_2\text{-Al}_2\text{O}_3$ coatings containing benzotriazole at three concentrations [62]

Samples	i_{corr} ($\mu\text{A}/\text{Cm}^2$)	β_a (V/dec)	β_c (V/dec)	E_{corr} (mV)	i_{pass} ($\mu\text{A}/\text{Cm}^2$)	η_p (%)
Titania–alumina (no benzotriazole)	16.6	0.668	0.277	−1149	36.3	–
Titania–alumina coating (1.2% benzotriazole)	20.4	0.710	0.332	−1135	56.2	−23
Titania–alumina coating (3.6% benzotriazole)	3.99	0.626	0.286	−1129	19.9	76
Titania–alumina coating (4.8% benzotriazole)	13.4	0.966	0.328	−1147	61.6	19

5.5 Zirconia Coating

Zirconia (ZrO_2) is one of the important ceramics with enhanced mechanical strength, thermal stability, wear, and corrosion resistances with an acceptable level of chemical stability and high hardness [86]. High degree of cracks happened in the coating of ZrO_2 prepared via sol–gel method is one of its main drawbacks and application of stabilizing agents can be effectively reduced this drawback. It's believed that these cracks form during the coating heat treatment due to stress formation. By in situ observing the gel film formation under heat treatment condition by Kozuka, it was revealed that the microscopic cracks formed in the heating-up stage and the starting temperature for the crack formation is highly depended on heating rate, film thickness, water-to-alkoxide ratio, and humidity. Via two methods, the film thickness can be increased without further crack development, (1) repetition of the coating procedure and (2) adding organic polymers [87]. The cracks and the non-homogeneity of the coating only containing ZrO_2 can be seen in Fig. 7. Zirconia single-component coating. These cracks formed during the heat treatment procedure and subsequently solvent evaporation, due to the high thermal expansion coefficient [88, 89]. The $\text{ZrO}_2\text{-BTA}$ hybrid coating shows a well-distributed, nanostructured, and crack-free structure with the benzotriazole as an inhibitor agent which its reaction with the coating components can prevent creation and development of cracks thereby resulting in a homogeneous nanostructured surface.

According to the polarization curves (Fig. 8), the coating function as a physical protective barrier to block electrochemical reactions and changes in polarization plots toward a more positive corrosion potential (E_{corr}) and lower corrosion current (i_{corr}) can be seen. Electrochemical changes are observed between the uncoated samples and coated samples as well. The cathodic nature and anodic part of the polarization plot of Al 2024 are changed by the sol–gel coatings. The $\text{ZrO}_2\text{-BTA}$ nanostructured coating shows a more positive corrosion potential and lower corrosion current density than the coatings and the corrosion resistance increases due to the anti-corrosive effects of benzotriazole. The coatings containing the appropriate concentration of benzotriazole blocks sites and increases the corrosion resistance by two steps. The first

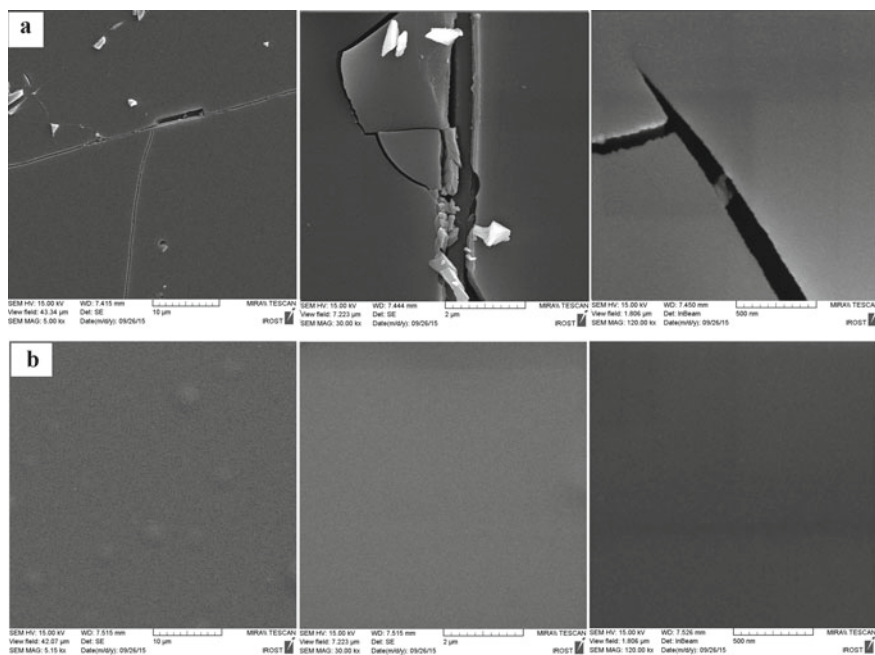


Fig. 7 FE-SEM images of the coatings deposited on Al 2024 alloy and heated at 150 °C for 2 h **a** ZrO_2 and **b** ZrO_2 -benzotriazole [89]

deterring effect reaches the metal–solution interface and then absorbs the inhibitor on the metal surface. The ceramic coating based on sol–gel, works like a dielectric material and the corrosion can be only started at the defects and flaws the presence in the coating. Hence, by diffusing the water and oxygen via the cracks and reaching the substrate surface, the corrosion can be started [89].

The Nyquist and Bode plots of Al 2024, ZrO_2 , and ZrO_2 -BTA nanostructured coatings in the 3.5 wt.% NaCl solution after immersion for 1 and 120 h (Fig. 9) confirm that the ZrO_2 coating has acceptable corrosion resistance and BTA in the zirconia coating enhances the resistance against corrosion. The hybrid coating showed better corrosion resistance compared to the inorganic one as its surface has lower level of flaws and imperfections. The sol–gel coatings corrode only through defects which allow the electrolyte to access the metal surface [89, 90]. The healing procedure can be seen normally through the polymerization reaction of the healing agent inside of the coating. Rupturing of the microcapsules containing the healing agents, during the crack formation lead to release of encapsulated compound and these compounds will go through the polymerization process when they contact with the catalyst. During exposure to water or moisture, the healing reaction proceeds by polymerization, cross-linking, or condensation to create a film to separate the metal substrate from the corrosive environment and consequently the corrosion process was reduced. Generally, The ZrO_2 -BTA nanostructured coating improves the corrosion

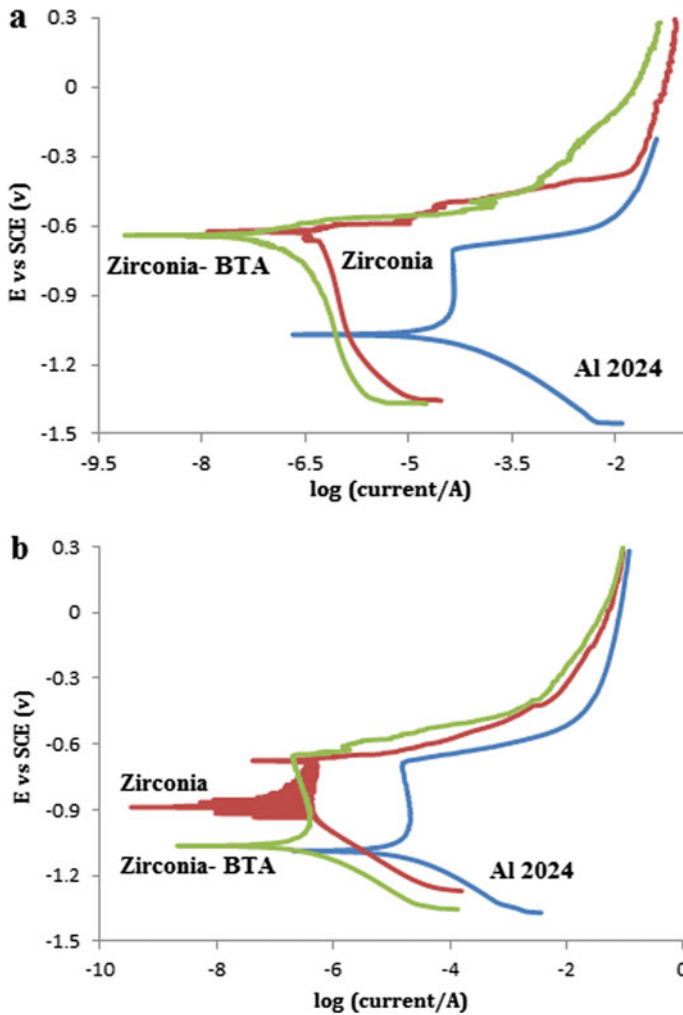


Fig. 8 Potentiodynamic polarization curves in the 3.5 wt.% NaCl solution of coatings: **a** 1 h and **b** 120 h [89]

resistance of the substrate in terms of corrosion potential, corrosion current density, passivity, and passive potential range, and the protection level of the ZrO_2 -BTA nanostructured coating is better than that of the inorganic ZrO_2 coating. In general, BTA improves the corrosion behavior of the ZrO_2 -BTA nanostructured coating in two ways by (1) formation of consistent and resilient coating from corrosion products and providing Warburg impedance and (2) formation of consistent and dense dual-layer to obstruct the ions and electrons movement at the interface of substrate and corrosive medium [90].

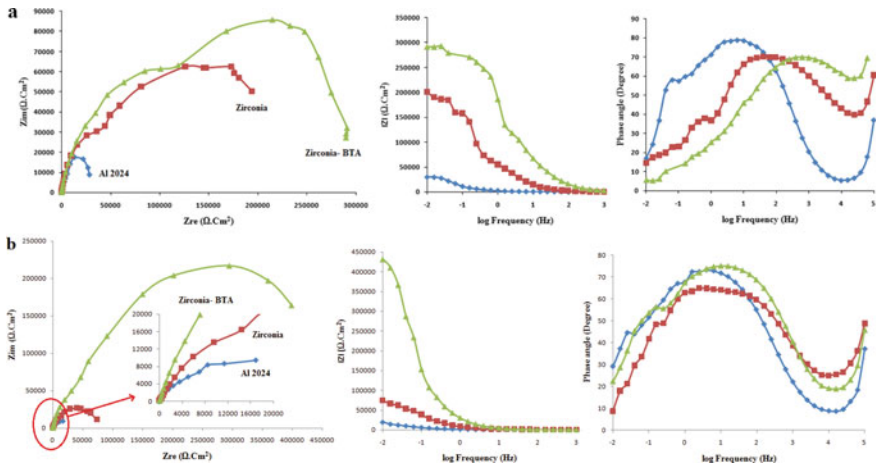


Fig. 9 Nyquist and bode-phase curves of the samples after immersion in the 3.5 wt. % NaCl solution for different times: **a** 1 h and **b** 120 h [89]

5.6 Zirconia–Alumina Composite Coatings

The mismatching of physical and chemical features of ZrO₂ and the substrate, Al 2024, is the reason for poor corrosion properties of this combination as the flaws can be created on ZrO₂ coating. By adding some compounds such as magnesium, yttrium and calcium oxides as stabilizer agents, the cubic and tetragonal phases will be more stable, and consequently, the harmful volume expansion due to transforming the tetragonal phase to monoclinic one will be prevented. Here, to enhance the behavior of ZrO₂ coating, Al₂O₃ is used to make the coating more stable and enhance its function [91–93].

According to the FE-SEM images showed in Fig. 10, cracks can be seen in the ZrO₂–Al₂O₃ coating (Fig. 10a) compared to the ZrO₂–Al₂O₃–benzotriazole coating (Fig. 10b), because of huge thermal expansion coefficient of ZrO₂ and removal of organic substances upon the heat treatment procedure. By performing the drying process in isopropanol and heat treatment procedure with a slower heating rate (1°C/min), crack propagation can be controlled [93, 94]. On the other hand, by using benzotriazole, no cracks and flaws would be seen due to the better ZrO₂–Al₂O₃–benzotriazole polymerization process. As shown in Fig. 10c–d, the elemental map of O confirms uniform distributions in the coatings. There is a larger percentage of oxygen and aggregation in the coating containing benzotriazole compared to the other coatings. One of the main roles of benzotriazole in smaller flaws is preventing crack propagation and its further development and therefore, providing flawless and crack-free coating [93–95]. Its mechanism of action is releasing the inhibitor into the cracks and by its reaction to the aluminum surface, protective [benzotriazole]ads:Al layer fills out the porosities. The thickness of the ZrO₂–Al₂O₃ and ZrO₂–Al₂O₃–benzotriazole coatings are 810 and 950 nm, respectively (Fig. 10 e–f).

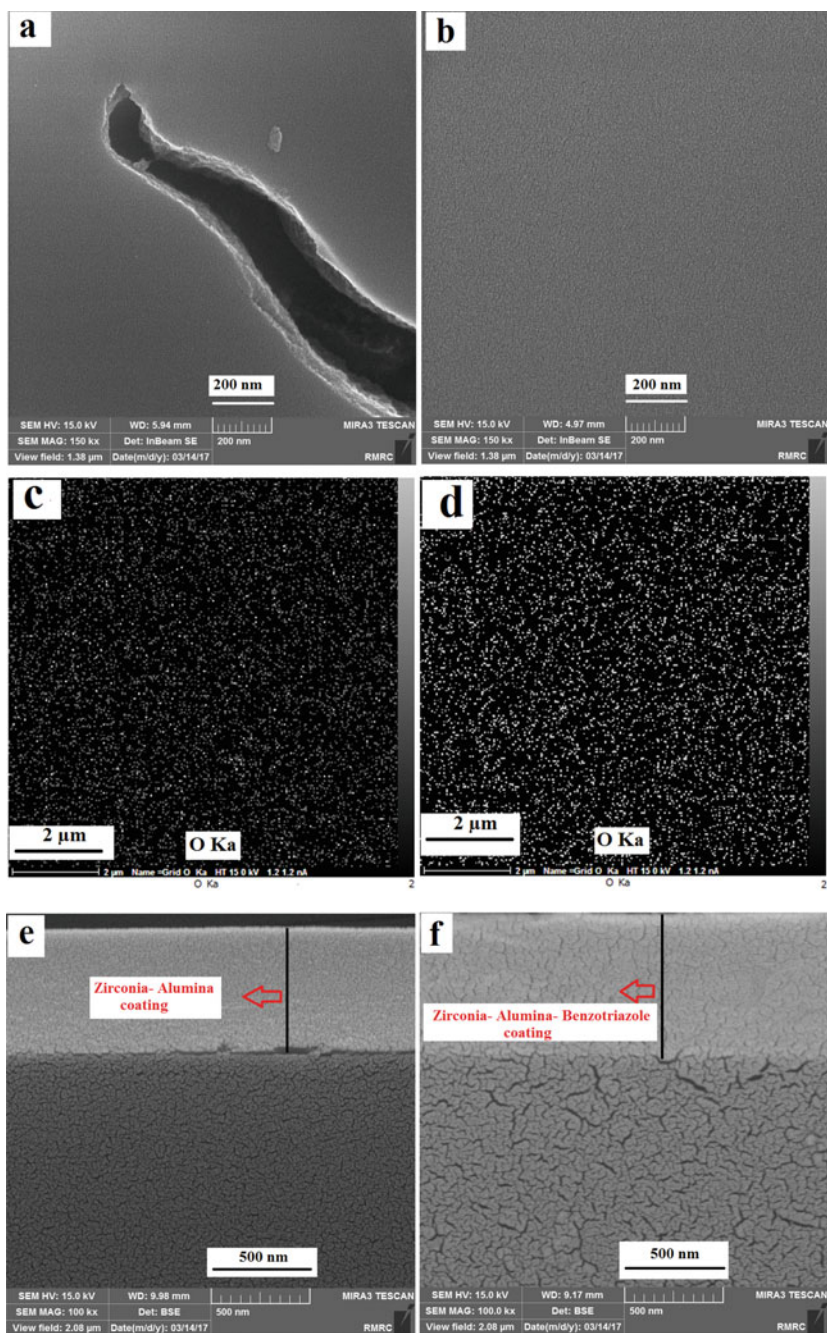


Fig. 10 FE-SEM images of **a** $\text{ZrO}_2\text{-Al}_2\text{O}_3$ coating, and **b** $\text{ZrO}_2\text{-Al}_2\text{O}_3\text{-benzotriazole}$; Elemental map of O acquired from **c** $\text{ZrO}_2\text{-Al}_2\text{O}_3$ coating, and **d** $\text{ZrO}_2\text{-Al}_2\text{O}_3\text{-benzotriazole}$ coating; FE-SEM cross-sectional images of **e** $\text{ZrO}_2\text{-Al}_2\text{O}_3$ coating, and **f** $\text{ZrO}_2\text{-Al}_2\text{O}_3\text{-benzotriazole}$ coating [93]

According to the Nyquist plots showed in Fig. 11, the dense $ZrO_2-Al_2O_3$ -benzotriazole coating shows better corrosion compared to the other groups. Although, there is a race between water absorption and chloride ions diffusion, however due to benzotriazole release, different behavior can be seen at different immersion time span. In this regard, after being immersed for 1–4 h, as this race is going on side by side, there is no difference between the corrosion resistance behavior of the different coatings. However, when the immersion time reached 6 h, excessive release of benzotriazole overcomes the other factors, water absorption and aggressive ions diffusion and thus, better corrosion resistance can be seen from $ZrO_2-Al_2O_3$ -benzotriazole coating.

The presence of some regions like Al_2Cu , Al_2CuMg , and Al_2Mg_3 , as the cathodic areas make the substrate, the Al 2204, more susceptible to intergranular corrosion. As the intergranular copper rich area would be dissolved, some sediments would be seen at the boundaries of corroded grains [84, 86]. According to the Nyquist plot

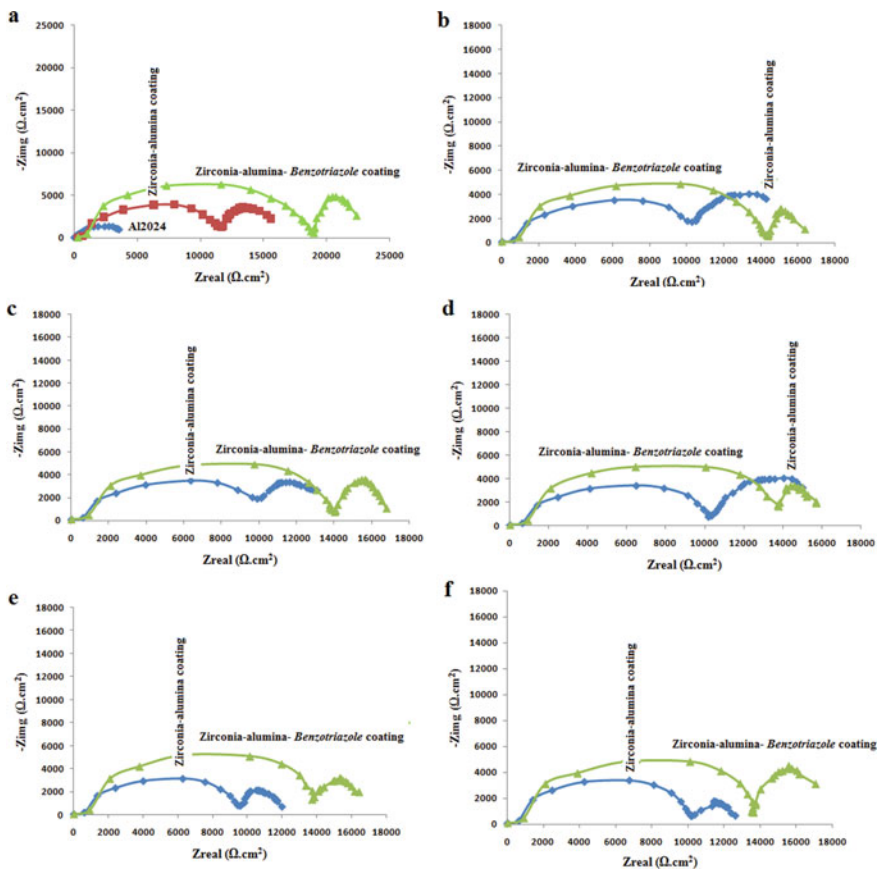


Fig. 11 Nyquist plots of the $ZrO_2-Al_2O_3$ and $ZrO_2-Al_2O_3$ -benzotriazole immersed for **a** 1 h, **b** 2 h, **c** 3 h, **d** 4 h, **e** 5 h, and **f** 6 h [93]

acquired from samples immersed for 1 h, the $\text{ZrO}_2\text{-Al}_2\text{O}_3$ coating hampered the galvanic corrosion and therefore improved the corrosion resistance. By extending the immersion time, due to water absorption and chloride ions diffusion within the cracks and flows, the corrosion resistance would be declined. benzotriazole relieves the cathodic and anodic reactions and also by hampering OH^- formation retains the neutrality of the solution exposed to the surface for longer time. Moreover, by forming corrosion products, the surface can be protected [62, 93–96]. Two mechanisms can be considered for zirconia–alumina–benzotriazole coating: (i) chloride ions diffusion prevention and adsorbing water via a homogenous coating without any crack (immersed for 1–4 h), and (ii) release of benzotriazole from the coating. As it can be seen in Fig. 11, benzotriazole mechanism of action is based on the below two states: (1) hampering cathodic reactions as a result of corrosion products creation via reaction with oxygen and (2) improving the double layer behavior developed between the surface of coating and solution (this enhancement can be verified due to improving the capacitance of double layer (C_{dl}) and the resistance between aqueous medium and the coating, after being immersed for 4–6 h) [93].

benzotriazole protects the surface of aluminum through formation of [benzotriazole]ads–Al layer. This can be explained by formation of BTA^- due to the loss of hydrogen from nitrogen in benzotriazole and its reaction with Al ions to form [benzotriazole]ads–Al [62, 93]. Many factors have impact of inhibitor molecules absorption, such as the functional group, electron density, π orbitals, as well as charged metal surface.

According to the graph acquired from the open circuit potentials (OCP) vs. time (Fig. 12), it can be seen that the potential for $\text{ZrO}_2\text{-Al}_2\text{O}_3\text{-benzotriazole}$, first shifted toward the positive direction followed by its negative shift. By application of benzotriazole, it can be seen from the polarization plot that the cathodic reaction was effectively hampered, delayed oxygen or OH^- reduction and consequently the corrosion of aluminum was prevented [62, 93]. Due to better protection on the case of $\text{ZrO}_2\text{-Al}_2\text{O}_3\text{-benzotriazole}$ coating compared to the $\text{ZrO}_2\text{-Al}_2\text{O}_3$, smaller potential fluctuation can be seen. The shifting of OCP to more positive values by extending the immersion period, can be a result of benzotriazole secretion into the medium. Though, the corrosion was prevented effectively due to the presence of stable and flawless $\text{ZrO}_2\text{-Al}_2\text{O}_3\text{-benzotriazole}$ coating and consequently the variation of OCP is small and insignificant.

6 Nanomechanical Properties

In addition to improving the corrosion behavior of ceramics-base coatings containing inhibitors by self-healing mechanisms, the mechanical properties of the coatings are of great importance. The intrinsic properties of ceramics such as high hardness lead to increased hardness and reduced flexibility of ceramic coatings, and usually different components of ceramic composite coatings lead to improved mechanical properties of the coatings. It has been shown that the alumina coating enhances the mechanical

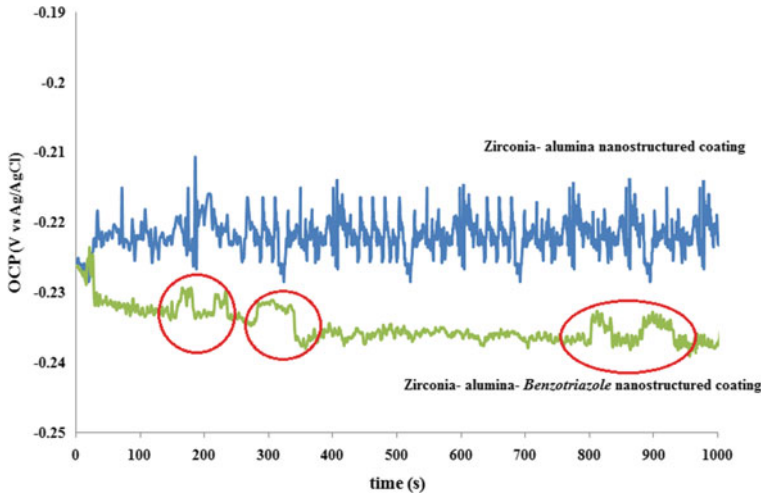


Fig. 12 Open circuit potential (OCP) versus immersion time for the $ZrO_2-Al_2O_3$ and $ZrO_2-Al_2O_3$ -benzotriazole coatings [93]

properties of sol-gel coatings on stainless steel or nitrided steel in terms of hardness and wear resistance, however, the tribological behavior of the coatings would be deteriorated due to the presence of cracks and defects. Adding ZrO_2 and TiO_2 to the coatings, decreased and increased the microhardness, respectively [97, 98]. benzotriazole in the nanostructured $ZrO_2-Al_2O_3$ -benzotriazole coating improves the corrosion resistance of Al 2024 with a protection efficiency of 76% [62]. Although, this enhancement is related to lower defects, however, a more comprehensive evaluation of the nanomechanical properties of hybrid ceramics-based coatings is necessary to understand the wear mechanism.

To evaluate the mechanical properties of the coatings, nanoindentation and nano-scratch tests are done. The curves and AFM images related to the nanoindentation tests at the applied loads of 50 and 60 μN are shown in Fig. 13 and the results, including hardness, elastic modulus and plastic deformation area are summarized in Table 3. Accordingly, results acquired for all the mentioned parameters are higher in the case of ZrO_2 compared to the $ZrO_2-Al_2O_3$ -benzotriazole ones at the load of 50 μN . These imperfections in the ZrO_2 coating cause higher energy absorption. At the load of 60 μN , the $ZrO_2-Al_2O_3$ -benzotriazole coating showed lower hardness while its elastic modulus and plastic deformation area are larger compared to the other groups. In general, by increasing the elastic modulus, dislocations movement will be harder and the reduction in hardness can be related to the organic compounds. The strengthening effect which has been seen in mechanical properties of $ZrO_2-Al_2O_3$ -benzotriazole coating is related to the solid solution formation [93, 94, 96].

At the load of 60 μN , not only the $ZrO_2-Al_2O_3$ -benzotriazole coating showed higher hardness and elastic modulus, but also, bigger plastic deformation area can

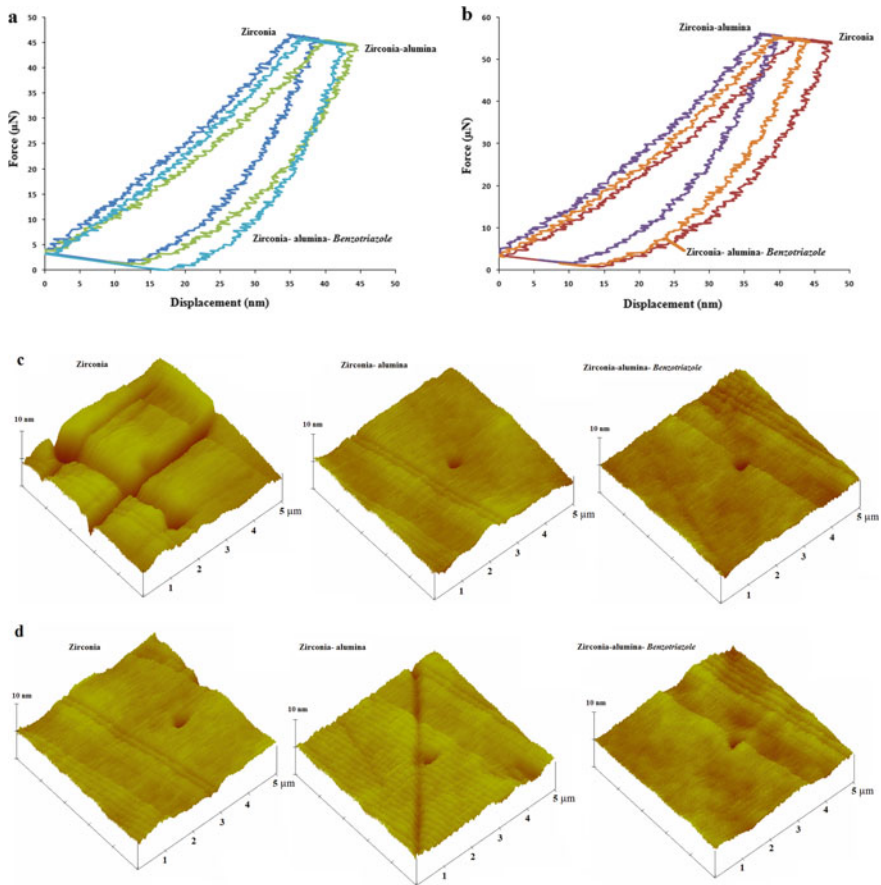


Fig. 13 Nanoindentation graphs for the coatings, exposed to two different loads: **a** 50 μN and **b** 60 μN ; AFM images after nanoindentation of the coatings at different loads: **c** 50 μN and **d** 60 μN [94]

Table 3 Coatings parameters acquired from the nanoindentation test at the loads of 50 and 60 μN [94]

Depth of penetration (nm)	Hardness (H) (GPa)	Elastic modulus (E) (GPa)	Coatings	Force (μN)
39	0.93	14	ZrO ₂	50
43	0.75	10.2	ZrO ₂ -Al ₂ O ₃	
42	0.69	15	ZrO ₂ -Al ₂ O ₃ -benzotriazole	
48	0.79	12.1	ZrO ₂	60
44	1.15	15	ZrO ₂ -Al ₂ O ₃	
45	0.91	13.8	ZrO ₂ -Al ₂ O ₃ -benzotriazole	

be seen compared to the ZrO_2 coating. Less defects, cracks free, uniform and integrated coatings improve the strength of the $ZrO_2-Al_2O_3$ coating compared to the ZrO_2 coating. As an organic compound, benzotriazole enhanced the behavior of the coating at the load of $60 \mu N$ by making a significant contribution to the reduction of hardness, elasticity and flexibility of the coating compared to the $ZrO_2-Al_2O_3$ coating. In fact, by increasing the tension and the applied force, the coatings' strength and solid solution formation are reduced and enhanced, respectively, due to the presence of benzotriazole. The coating hardness and elasticity would be decreased by increasing the force from 50 to $60 \mu N$. By applying higher load, defects play a more prominent role and make the dislocations to move easier in the ZrO_2 coating, as it can be concluded from the nanoindentation plot and maximum penetration depth. The $ZrO_2-Al_2O_3$ -benzotriazole coating shows a dissimilar behavior compared to the ZrO_2 coating, as the hardness and elastic modulus increased by elevating the applied force from 50 to $60 \mu N$, although those would be decreased at the deepest depth of penetration and also in the horizontal part of the nanoindentation graph. The elastic modulus of $ZrO_2-Al_2O_3$ coating is lower than the ZrO_2 coating at the applied load of $50 \mu N$, however by increasing the applied force to $60 \mu N$, the penetration depth would be increased. The higher force affects a larger area and the dislocations movements are hampered by the $ZrO_2-Al_2O_3$ solid solution [94, 96].

The mechanical behavior is assessed via the nanoscratch test. The image of the scratch and the roughness of ZrO_2 , $ZrO_2-Al_2O_3$, and $ZrO_2-Al_2O_3$ -benzotriazole at 50 and $60 \mu N$ (Fig. 14) indicate that both the ZrO_2 and $ZrO_2-Al_2O_3$ coatings show a more apparent plasticity encountered to indentation by increasing the load from 50 to $60 \mu N$, as shown by surface roughness plot in the movement path of indentation. It can be due to the sluggish dislocation movement at the load of $50 \mu N$. Under a load of $60 \mu N$, plastic deformation and dislocations movement causes a shrinkage at the end of the indenter path. Such shrinking, and also groove edges rounding represent the high plastic deformability for the coating with benzotriazole at the load of $50 \mu N$. Two interesting points can be seen in the $ZrO_2-Al_2O_3$ -benzotriazole coating friction coefficient at the load of $60 \mu N$. These repeatable fluctuations stemmed from the homogeneity of coating properties throughout the indenting path and the rise and fall of the friction coefficient can be explained by even distribution of benzotriazole in the coating.

Benzotriazole increases the flexibility of the coating and plays a dominant role in wear adhesion. By roughness increasing and the $ZrO_2-Al_2O_3$ -benzotriazole shrinkage through the path of indentation, friction coefficient was first increased and then decreased. In general, alumina increases the ability of plastic deformation and impedes movement of dislocations, whereas the flexibility was increased due to benzotriazole, since the coating was piled up at the edge and at the end of the friction path [99–102].

Figure 15 illustrates that the average friction coefficients of the ZrO_2 , $ZrO_2-Al_2O_3$, and $ZrO_2-Al_2O_3$ -benzotriazole coatings are 0.38 , 0.32 , and 0.29 under a load of $50 \mu N$, and 0.48 , 0.51 , and 0.41 under $60 \mu N$. According to the wear curves and the coatings diagram for surface roughness at the load below $50 \mu N$, abrasion with plowing can be seen as the dominant mechanism. The elastic and plastic deformation

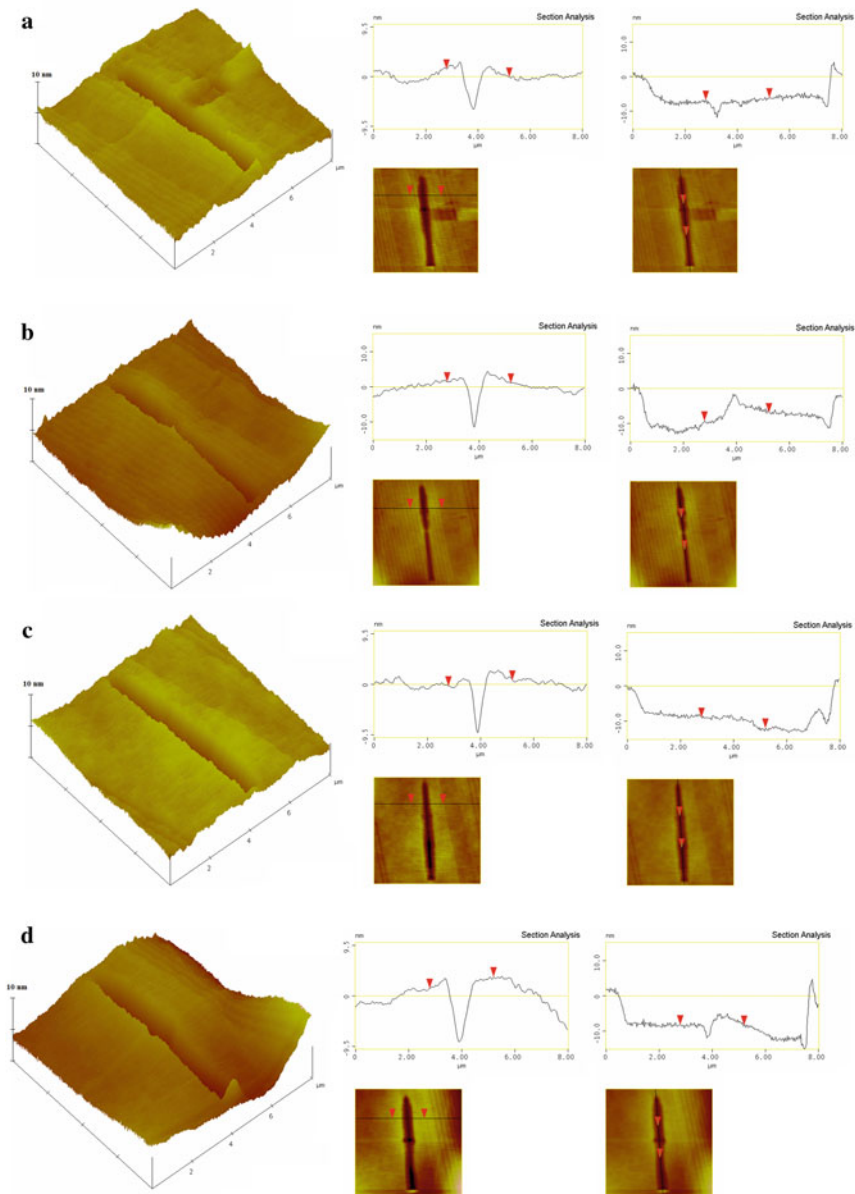


Fig. 14 The AFM image of the nanoscratched area and its relative surface roughness by applying 50 μN load on **a** ZrO_2 , **b** $\text{ZrO}_2\text{-Al}_2\text{O}_3$, and **c** $\text{ZrO}_2\text{-Al}_2\text{O}_3\text{-benzotriazole}$ coatings, and 60 μN load on: **d** ZrO_2 , **e** $\text{ZrO}_2\text{-Al}_2\text{O}_3$, and **f** $\text{ZrO}_2\text{-Al}_2\text{O}_3\text{-benzotriazole}$ coating [94]

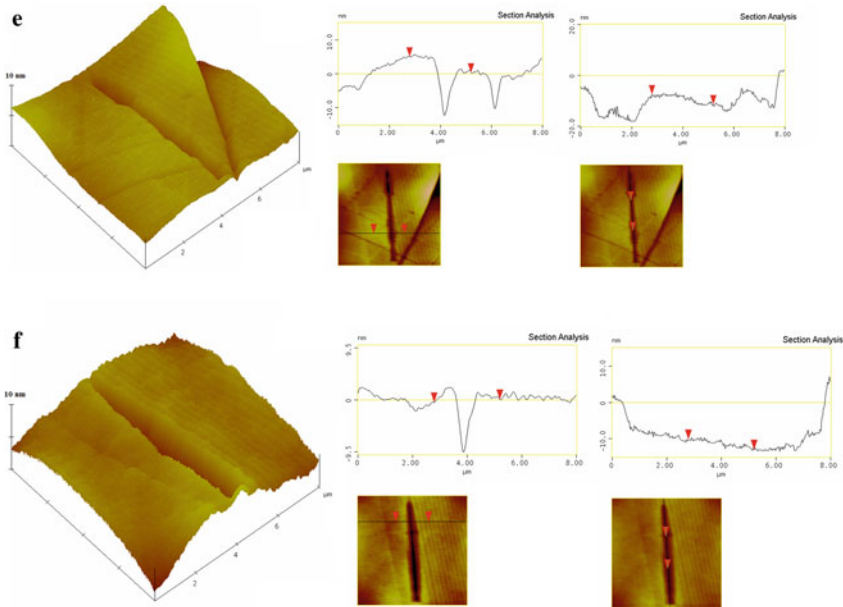


Fig. 14 (continued)

the plowing phenomenon, which can act as barriers throughout the wear test thus giving rise to larger friction coefficients for the $ZrO_2-Al_2O_3$ -benzotriazole coating. One method to reduce the friction coefficients and improve the wear behavior is to increase the hardness of the surface and in this regard, the ZrO_2 coating has the lowest friction coefficient due to the largest hardness under $50 \mu N$ [94].

$50 \mu N$ load may not apply sufficient plastic deformation and so abrasion is the dominant wear mechanism. In the beginning, small plastic deformation occurs in the indentation path due to tensions caused by the formation of the homogeneous and uniform coating. In comparison, as the adhesion can be seen in the wear area of $ZrO_2-Al_2O_3$ -benzotriazole coating, it can be said that the dominant wear mechanism is adhesion [94]. By increasing the load to $60 \mu N$, the dominant mechanism is changed to the abrasion with shear for the $ZrO_2-Al_2O_3$ and $ZrO_2-Al_2O_3$ -benzotriazole coatings, and the proof for this fact is the noticeable peaks and valleys in the wear graphs, especially the one with benzotriazole. As the strength of $ZrO_2-Al_2O_3$ is higher compared to the $ZrO_2-Al_2O_3$ -benzotriazole and the $60 \mu N$ load has an influence on dislocation movement, the former one has higher indentation resistance.

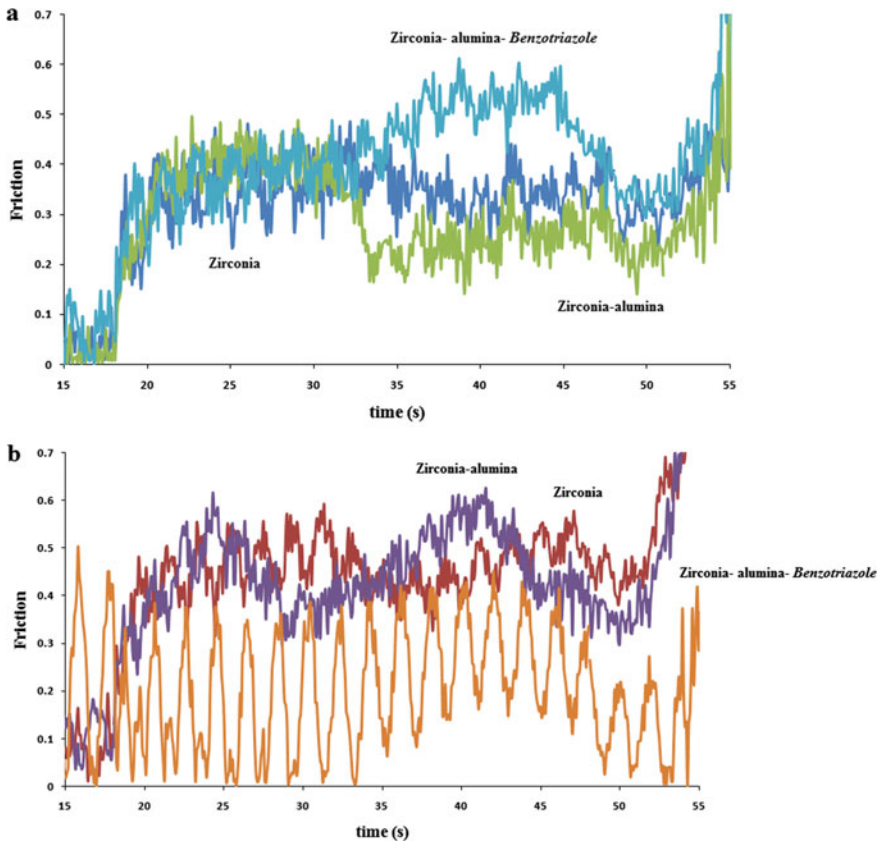


Fig. 15 Friction coefficients graphs of the ZrO_2 , $ZrO_2-Al_2O_3$, and $ZrO_2-Al_2O_3$ -benzotriazole coatings under **a** 50 μN , and **b** 60 μN [94]

7 Conclusion and New Perspective

Much effort has been made to develop self-healing coatings with high corrosion resistance and desirable mechanical properties in order to increase the lifetime of metallic components. In particular, ceramic coatings are widely used in the industry due to the high hardness, low friction, high corrosion resistance, and robust chemical resistance, but cracking and porosity reduce the corrosion resistance leading to possible failure in the field. In this respect, self-healing agents can be incorporated into the structure to increase the properties and longevity. Incorporation of repairing agents into ceramic coatings increases the corrosion resistance by leaving repairing agents at defects such as cavities and cracks, and the reactions with oxygen and moisture produce corrosion products that facilitate repair at defects. The proper choice of the inhibiting polymers and their products increases the flexibility and strength of the ceramic coatings along with enhanced corrosion resistance. However, it should be

mentioned that these materials are still in the experimental stage and more research is required to bring the technology to industrial fruition.

At present, existing technologies for designing self-healing materials are expensive, which has hampered the widespread usage of the materials for various common applications, and with the spread of science, it is expected that new advancement will make the use of self-healing materials possible in everyday life. In future, one of the most important applications of ceramic-based self-healing materials can be their use in biomaterials along with using natural and biocompatible inhibitors so that biocompatible ceramic-based self-healing composites can improve durability of artificial bones, dentures, and so on.

References

1. I. Gonzalez-Torre, J. Norambuena-Contreras, *Constr. Build. Mater.* **258**, 119568 (2020)
2. S.K. Ghosh (ed.), *Self-Healing Materials: Fundamentals, Design Strategies, and Applications* ed. by S.K. Ghosh (Wiley, Weinheim, 2009). pp. 1–25
3. W. Wang, N.G. Moreau, Y. Yuan, P.R. Race, W. Pang, *Comput. Mater. Sci.* **168**, 180 (2019)
4. P. Fratzl, R. Weinkamer, in *Self Healing Materials: An Alternative Approach to 20 Centuries of Materials Science*, edited by S. van der Zwaag (Springer, 2007), pp. 323–335
5. F.J. Vermolen, W.G. van Rossum, E. Javierre, J.A. Adam, in *Self Healing Materials: An Alternative Approach to 20 Centuries of Materials Science*, edited by S. van der Zwaag (Springer, 2009), pp. 337–363
6. M.R. Kessler, *Proc. Inst. Mech. Eng. Part G J. Aerosp. Eng.* **221**, 479 (2007)
7. W. Zhang, Q. Zheng, A. Ashour, B. Han, *Compos. Part B Eng.* **189**, 107892 (2020)
8. K. Li, Z. Liu, C. Wang, W. Fan, F. Liu, H. Li, Y. Zhu, H. Wang, *Prog. Org. Coatings* **145**, 105668 (2020)
9. H. Li, Y. Feng, Y. Cui, Y. Ma, Z. Zheng, B. Qian, H. Wang, A. Semenov, D. Shchukin, *Prog. Org. Coatings* **145**, 105684 (2020)
10. A.G. Cordeiro Neto, A.C. Pellanda, A.R. de Carvalho Jorge, J.B. Floriano, M.A. Coelho Berton, *Prog. Org. Coatings* **147**, 105874 (2020)
11. S.K. Ghosh, *Functional Coatings by Polymer Microencapsulation*, ed. by S.K. Ghosh (Wiley, Weinheim, 2006), pp. 1–28
12. S. Javadian, Z. Ahmadvan, A. Yousefi, *Prog. Org. Coatings* **147**, 105678 (2020)
13. S. Xu, J. Li, H. Qiu, Y. Xue, J. Yang, *Compos. Commun.* **19**, 220 (2020)
14. S.R. White, N.R. Sottos, P.H. Geubelle, J.S. Moore, M.R. Kessler, S.R. Sriram, E.N. Brown, S. Viswanathan, *Nature* **409**, 794 (2001)
15. A. Danish, M.A. Mosaberpanah, M. Usama Salim, *J. Mater. Res. Technol.* **9**, 6883 (2020)
16. D. Mohanty, A. Sil, K. Maiti, *Ceram. Int.* **37**, 1985 (2011)
17. F. Tavangarian, D. Hui, G. Li, *Compos. Part B Eng.* **144**, 56 (2018)
18. L. Restuccia, A. Reggio, G.A. Ferro, J.M. Tulliani, *Procedia Struct. Integr.* **3**, 253 (2017)
19. F. Awaja, S. Zhang, M. Tripathi, A. Nikiforov, N. Pugno, *Prog. Mater. Sci.* **83**, 536 (2016)
20. B.S. Kim, K. Ando, M.C. Chu, S. Saito, *J. Soc. Mater. Sci. Jpn.* **52**, 667 (2003)
21. K. Ando, B.-S. Kim, S. Kudama, S.-P. Liu, K. Takahashi, S. Saito, *Journal* **52**, 1464 (2003)
22. W. Nakao, T. Osada, K. Yamane, K. Takahashi, K. Ando, *J. Jpn. Inst. Met.* **69**, 663 (2005)
23. CHASE and M.W., *J. Phys. Chem. Reference Data* **1529** (1998)
24. M. Nosonovsky, B. Bhushan, *Mater. Sci. Eng. R. Rep.* **58**, 162 (2007)
25. M. Nosonovsky, S.K. Esche, *Entropy* **10**, 49 (2008)
26. F. Zhang, P. Ju, M. Pan, D. Zhang, Y. Huang, G. Li, X. Li, *Corros. Sci.* **144**, 74 (2018)
27. G. Mu, X. Li, Q. Qu, J. Zhou, *Corros. Sci.* **48**, 445 (2006)

28. A.E. Hughes, in *Recent Advances in Smart Self-Healing Polymers and Composites*, ed. by G. Li, H.B.T.-R.A. in S.S.P. and C. Meng (Woodhead Publishing, 2015), pp. 211–241
29. C. Monticelli, in *Encyclopedia of Interfacial Chemistry: Surface Science and Electrochemistry*, Vol. 6, ed. by K. Wandelt (Elsevier, 2018), pp. 164–171
30. Y. Morozov, L.M. Calado, R.A. Shakoor, R. Raj, R. Kahraman, M.G. Taryba, M.F. Montemor, *Corros. Sci.* **159**, 108128 (2019)
31. Y. Su, S. Qiu, D. Yang, S. Liu, H. Zhao, L. Wang, Q. Xue, *J. Hazard. Mater.* **391**, 122215 (2020)
32. L.B. Coelho, E.B. Fava, A.M. Kooijman, Y. Gonzalez-Garcia, M.-G. Olivier, *Corros. Sci.* **175**, 108893 (2020)
33. D. Li, F. Wang, X. Yu, J. Wang, Q. Liu, P. Yang, Y. He, Y. Wang, M. Zhang, *Prog. Org. Coat.* **71**, 302–309 (2011)
34. R.B. Figueira, R. Sousa, C.J.R. Silva, in *Advances in Smart Coatings and Thin Films for Future Industrial and Biomedical Engineering Applications*, ed. by A.S.H. Makhlof and N. Y. B. T.-A. in S. C. and T. F. for F. I. and B. E. A. Abu-Thabit (Elsevier, 2020), pp. 57–97
35. P. Wang, X. Dong, D.W. Schaefer, *Corros. Sci.* **52**, 943–949 (2010)
36. C. Verma, E.E. Ebenso, M.A. Quraish, *J. Mol. Liq.* **316**, 113874 (2020)
37. F. Ubaid, A.B. Radwan, N. Naem, R.A. Shakoor, Z. Ahmad, M.F. Montemor, R. Kahraman, A.M. Abdullah, A. Soliman, *Surf. Coatings Technol.* **372**, 121 (2019)
38. S.A. Umoren, U.M. Eduok, *Carbohydr. Polym.* **140**, 314 (2016)
39. L.P. Kazansky, I.A. Selyaninov, Yu.I. Kuznetsov, *Appl. Surf. Sci.* **258**, 6807–6813 (2012)
40. Y. Chen, B. Ren, S. Gao, R. Cao, *J. Colloid Interface Sci.* **565**, 436–448 (2020)
41. H. Shi, F. Liu, E. Han, *Mater. Chem. Phys.* **124**, 291 (2010)
42. T. Hack, D. Raps, R. Supplitt, U. Schubert, US 8,361,627 B2 (2013)
43. N.P. Tavandashiti, S. Sanjabi, *Prog. Org. Coatings* **69**, 384 (2010)
44. S.B. Ulaeto, R. Rajan, J.K. Pancreicious, T.P.D. Rajan, B.C. Pai, *Prog. Org. Coatings* **111**, 294 (2017)
45. D.G. Shchukin, H. Möhwald, *Small* **3**, 926 (2007)
46. M. Toorani, M. Aliofkhaezai, A. Sabour Rouhaghdam, *Surf. Coatings Technol.* **352**, 561 (2018)
47. A.F. Jaramillo, L.F. Montoya, J.M. Prabhakar, J.P. Sanhueza, K. Fernández, M. Rohwerder, D. Rojas, C. Montalba, M.F. Melendrez, *Prog. Org. Coatings* **135**, 191 (2019)
48. A. Conde, A. Durán, J.J. de Damborenea, *Prog. Org. Coatings* **46**, 288 (2003)
49. X. Zhang, Y. Lv, S. Fu, Y. Wu, X. Lu, L. Yang, H. Liu, Z. Dong, *Mater. Sci. Eng. C* **117**, 111321 (2020)
50. M.L. Zheludkevich, R. Serra, M.F. Montemor, I.M.M. Salvado, M.G.S. Ferreira, *Surf. Coatings Technol.* **200**, 3084 (2006)
51. A. Ghafari, M. Yousefpour, A. Shanaghi, *Appl. Surf. Sci.* **465**, 427 (2019)
52. L.S. Živković, B.V. Jegdić, V. Andrić, K.Y. Rhee, J.B. Bajat, V.B. Mišković-Stanković, *Prog. Org. Coatings* **136**, 105219 (2019)
53. S.M. Dezfuli, M. Sabzi, *Int. J. Appl. Ceram. Technol.* **15**(5), 1248–1260 (2018)
54. H. Pulikkalparambil, S. Siengchin, J. Parameswaranpillai, *Nano-Struct. Nano-Objects* **16**, 381–395 (2018)
55. R. Corriu, T.A. Nguyễn, *Molecular Chemistry of Sol-Gel Derived Nanomaterials* (Wiley Online Library, 2009)
56. A.K. Zak, W.H.A. Majid, *Ceram. Int.* **37**, 753 (2011)
57. S.M. Madani, M. Ehteshamzadeh, H.H. Rafsanjani, S.S. Mansoori, *Mater. Corros.* **61**, 318 (2010)
58. A. Stankiewicz, I. Szczygieł, B. Szczygieł, *J. Mater. Sci.* **48**, 8041 (2013)
59. K. Yasakau, *Active Corrosion Protection of AA2024 by Sol-Gel Coatings with Corrosion Inhibitors* (Universidade de Aveiro, 2011)
60. A. Shanaghi, M. Kadkhodaie, *Corros. Eng. Sci. Technol.* **52**, 332 (2017)
61. A. Shanaghi, P.K. Chu, H. Moradi, *Surf. Rev. Lett.* **24**, 1 (2017)
62. M.S. Sharifiyan, A. Shanaghi, H. Moradi, P.K. Chu, *Surf. Coatings Technol.* **321**, 36 (2017)

63. M. Farahani, H. Yousefnia, Z.S. Seyedraoufi, Y. Shajari, *Ceram. Int.* **45**(13), 16584–16590 (2019)
64. D. Wang, G.P. Bierwagen, *Prog. Org. Coatings* **64**, 327 (2009)
65. K.H. Wu, T.C. Chang, C.C. Yang, G.P. Wang, *Thin Solid Films* **513**, 84 (2006)
66. E.D. Mekeridis, I.A. Kartsonakis, G.C. Kordas, *Prog. Org. Coatings* **73**, 142 (2012)
67. H. Hassannejad, T. Shahrabi, F. Malekmohammadi, A. Shanaghi, M. Aliofkhaezrai, A. Oskuie, *Curr. Appl. Phys.* **10**, 1022 (2010)
68. D. Zare Hossein Abadi, A. Ershad Langroudi, A. Rahimi, *J. Colour Sci. Technol.* **3**, 121 (2009)
69. H.-L. Wang, H.-P. Qi, X.-N. Wei, X.-Y. Liu, W.-F. Jiang, *Chin. J. Catal.* **37**, 2025 (2016)
70. G.C.C. Yang, C.-J. Li, *Desalination* **200**, 74 (2006)
71. G.X. Shen, Y.C. Chen, C.J. Lin, *Thin Solid Films* **489**, 130 (2005)
72. X. Nie, E.I. Meletis, J.C. Jiang, A. Leyland, A.L. Yerokhin, A. Matthews, *Surf. Coatings Technol.* **149**, 245 (2002)
73. C.G. Darive, A.F. Galio, in *Dev. Corros. Prot.*, ed. by M. Aliofkhaezrai (INTECH, 2014), pp. 365–379
74. M.R. Mohammadi, *Mater. Sci. Semicond. Process.* **27**, 711 (2014)
75. X. Du, K. Men, Y. Xu, B. Li, Z. Yang, Z. Liu, L. Li, L. Li, T. Feng, W. ur Rehman, I. Ullah, S. Mao, *J. Colloid Interface Sci.* **443**, 170 (2015)
76. K. Kadrigama, M.M. Noor, N.M. Zuki, M.M. Rahman, M.R.M. Rejab, R. Daud, K.A. Abou-El-Hossein, *Jordan J. Mech. Ind. Eng.* **2**, 209 (2008)
77. S.A. Yero, M.R. Hainin, H. Yacoob, *Ijrras* **13**, 98 (2012)
78. G. Quintana, M.L. Garcia-Romeu, J. Ciurana, *J. Intell. Manuf.* **22**, 607 (2011)
79. A.K. Mainjot, A. Najjar, B.D. Jakubowicz-Kohen, M.J. Sadoun, *Dent. Mater.* **31**, 1142 (2015)
80. H.-C. Yu, S.B. Adler, S.A. Barnett, K. Thornton, *Electrochim. Acta* **354**, 136534 (2020)
81. S. Darwich, *Corrosion Protection Concepts for Aluminium and Magnesium Alloys Coated with Silica Films Prepared by Water-Based Sol-Gel Process* (Technischen Universitat Chemnitz, 2012)
82. A.R. Simbar, A. Shanaghi, H. Moradi, P.K. Chu, *Mater. Chem. Phys.* **240**, 122233 (2020)
83. K.F. Khaled, *Electrochim. Acta* **48**, 2493 (2003)
84. J. Aljourani, K. Raeissi, M.A. Golozar, *Corros. Sci.* **51**, 1836 (2009)
85. D. Laouali, F. Bénière, *J. Mater. Environ. Sci.* **3**, 34 (2012)
86. S. Saridag, O. Tak, G. Alniacik, *World J. Stomatol.* **2**, 40 (2013)
87. S. Sakka, in *Handbook of Advanced Ceramics. Materials, Applications, Processing, and Properties*, ed. by S. Somiya, 2nd ed. (Academic Press, 2013), pp. 1–17
88. L. Paussa, N.C. Rosero Navarro, D. Bravin, F. Andreatta, A. Lanzutti, M. Aparicio, A. Durán, L. Fedrizzi, *Prog. Org. Coatings* **74**, 311 (2012)
89. S.M. Dezfuli, A. Shanaghi, S. Baghshahi, *Prot. Met. Phys. Chem. Surfaces* **54**, 1050 (2018)
90. E. Setare, K. Raeissi, M.A. Golozar, M.H. Fathi, *Corros. Sci.* **51**, 1802 (2009)
91. M.A. Domínguez-Crespo, A. García-Murillo, A.M. Torres-Huerta, F.J. Carrillo-Romo, E. Onofre-Bustamante, C. Yáñez-Zamora, *Electrochim. Acta* **54**, 2932 (2009)
92. E. Celik, I. Keskin, I. Kayatekin, F. Ak Azem, E. Özkan, *Mater. Charact.* **58**, 349 (2007)
93. A. Shanaghi, A.R. Sourì, P.K. Chu, *J. Alloys Compd.* **816**, 152662 (2020)
94. A. Shanaghi, A.R. Sourì, M. Rafie, P.K. Chu, *Thin Solid Films* **689**, 137417 (2019)
95. S.M. Dezfuli, M. Sabzi, *Adv. Mater. Technol.* **7**(4), 75–92 (2019)
96. A. Shanaghi, A.R. Sourì, M. Rafie, P.K. Chu, *Appl. Phys. A Mater. Sci. Process.* **125**, 1 (2019)
97. R. Younes, M.A. Bradai, A. Sadeddine, Y. Mouadji, A. Bilek, A. Benabbas, *Trans. Nonferrous Met. Soc. China* **26**, 1345 (2016)
98. B.J. McEntire, B.S. Bal, M.N. Rahaman, J. Chevalier, G. Pezzotti, *J. Eur. Ceram. Soc.* **35**, 4327 (2015)

99. N. Zotov, M. Bartsch, G. Eggeler, *Surf. Coatings Technol.* **203**, 2064 (2009)
100. M.G. Ahangari, A. Fereidoon, *Mater. Chem. Phys.* **151**, 112 (2015)
101. A. Shanaghi, A.R.S. Rouhaghdam, S. Ahangarani, P.K. Chu, *Mater. Res. Bull.* **47**, 2200 (2012)
102. J. Sun, C. Liu, R. Zhang, F. Gong, C. Wang, G. Li, *Ceram. Ceram. Inter.* **45**(10), 13597–13604 (2019)